

VERSAT - S2D & VERSAT - D2D

Version 2019.10.3 with PSPA & [C]_{a,b} modules

STATIC AND DYNAMIC 2-DIMENSIONAL FINITE ELEMENT ANALYSIS OF CONTINUA

- Microsoft .NET Framework 3.5
- Microsoft Windows XP, & Windows 7 & Windows 10

Volume 1: TECHNICAL MANUAL

© 1998 – 2020 Dr. G. WU

© 1998 – 2020 Wutec Geotechnical International (WGI), B.C., Canada

Website: <http://www.wutecgeo.com>

LIMITATION OF LIABILITY

The following terms and conditions with regard to limitation of liability must be accepted to proceed with the use of VERSAT-2D.

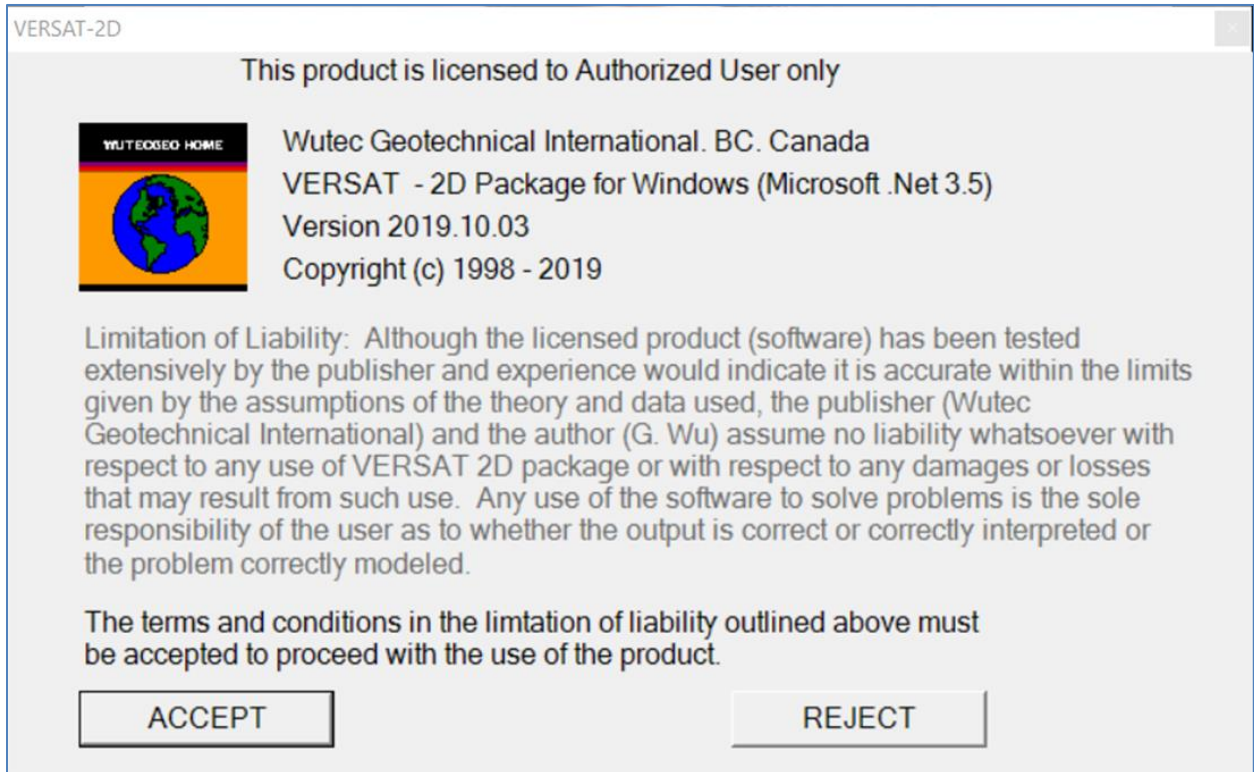


TABLE OF CONTENTS

	<u>Page</u>
LIMITATION OF LIABILITY	I
1.0 INTRODUCTION	1
2.0 VERSAT-S2D TECHNICAL MANUAL	4
2.1 INTRODUCTION	4
2.2 LINEAR ELASTIC MODEL	4
2.3 PLASTICITY STRENGTH MODELS FOR SOIL AND ROCK	5
2.3.1 <i>Mohr - Coulomb SAND Model</i>	5
2.3.2 <i>Von - Mises CLAY Model</i>	5
2.3.3 <i>Shear Strength Models for Silts</i>	7
2.4 STRESS LEVEL DEPENDENT STIFFNESS PARAMETERS.....	7
2.5 BENDING ELEMENTS FOR STRUCTURAL MEMBERS.....	7
2.6 SPRING ELEMENTS FOR STRUCTURAL MEMBERS.....	8
2.7 PORE WATER PRESSURE AND EFFECTIVE STRESSES	9
2.8 CALCULATION OF STRESSES AND DEFORMATIONS CAUSED BY STRAIN-SOFTENING OF SOILS	10
2.9 UPDATED LAGRANGIAN ANALYSIS	10
2.10 FACTORS OF SAFETY	10
2.11 GRAVITY ON AND OFF.....	11
2.12 UNITS AND SIGNS	11
3.0 VERSAT-D2D TECHNICAL MANUAL	12
3.1 SYSTEM EQUATIONS OF MOTIONS AND MODAL FREQUENCIES	12
3.1.1 <i>Equations of Motions</i>	12
3.1.2 <i>Modal Frequencies and Periods</i>	12
3.2 VISCOUS DAMPING.....	13
3.2.1 <i>System Damping for Global Structure</i>	13
3.2.2 <i>Viscous Damping for Local Structure</i>	14
3.3 LINEAR ELASTIC MODEL	14
3.4 NONLINEAR HYPERBOLIC STRESS - STRAIN MODEL.....	15
3.4.1 <i>Low - Strain Stiffness Parameters</i>	15
3.4.2 <i>Hyperbolic Shear Stress-Strain Model</i>	15
3.4.3 <i>Determination of Ultimate Shear Stress</i>	16
3.4.4 <i>Hysteretic Damping in a Hyperbolic Model</i>	17
3.5 SAND MODEL - DYNAMIC PORE WATER PRESSURE MODELS	18
3.5.1 <i>Introduction</i>	18
3.5.2 <i>Plastic Volumetric Strain</i>	19
3.5.3 <i>Martin-Finn-Seed's Pore Water Pressure Model</i>	19
3.5.4 <i>Modified MFS Pore Water Pressure Model</i>	20
3.5.5 <i>Seed's Pore Water Pressure Model</i>	22
3.6 EFFECTIVE STRESS DYNAMIC ANALYSIS	25
3.6.1 <i>Factors of Safety against Soil Liquefaction</i>	26
3.6.2 <i>Dynamic Pore Water Pressure Ratio: r_u</i>	26
3.6.3 <i>Reduction of Stiffness by Dynamic Pore Water Pressure</i>	26
3.6.4 <i>Behavior of Liquefied Soils</i>	27
3.7 DETERMINATION OF SHEAR STRENGTH AND MAXIMUM SHEAR STRESS	28
3.7.1 <i>Mohr-Coulomb SAND Model:</i>	28
3.7.2 <i>Constant Strength CLAY Model:</i>	29
3.7.3 <i>Maximum Static Plus Dynamic Shear Stress</i>	29
3.7.4 <i>Maximum Shear Strain</i>	30
3.8 BENDING ELEMENTS FOR STRUCTURAL MEMBERS.....	30
3.9 SPRING ELEMENTS FOR STRUCTURAL TRUSS OR BAR	31
3.10 UPDATED LAGRANGIAN ANALYSIS	31
3.11 GRAVITY ON AND OFF.....	31



3.12	BOUNDARY CONDITIONS	32
3.12.1	<i>Fixed Boundary</i>	32
3.12.2	<i>Free-Field Stress Boundary</i>	32
3.12.3	<i>Constrained Displacement Boundary</i>	32
3.13	DYNAMIC POINT LOADS	33
3.14	DYNAMIC ANALYSIS OF 1D SOIL COLUMNS.....	33
3.15	UNITS AND SIGNS	33
3.16	DYNAMIC ANALYSIS OF UPPER SAN FERNANDO DAM UNDER 1971 EARTHQUAKE	33
4.0	ADVANCED OPTIONS FOR VERSAT-2D DYNAMIC ANALYSIS	34
4.1	OUTCROPPING VELOCITY INPUT	34
4.1.1	<i>Equation of Motions and its Formulations</i>	34
4.1.2	<i>Traveling of Input Motion at the Viscous Base</i>	37
4.1.3	<i>An Example Using Outcropping Velocity Input and Comparing with SHAKE</i>	37
4.2	SILT MODEL - UPDATED IN v.2016.6.18	39
4.2.1	<i>Shear Stress - Strain Relationship for SILT Model</i>	39
4.2.2	<i>Shear Strengths for SILT Model</i>	40
4.2.3	<i>Dynamic Pore Water Pressures and Liquefaction for SILT Model</i>	40
4.2.4	<i>Post Liquefaction Simulation for SILT model</i>	40
4.3	PROBABILISTIC SEISMIC PERFORMANCE ANALYSIS (PSPA).....	43
4.3.1	<i>PSPA Method (version 2019.05 and later)</i>	43
4.3.2	<i>Input and Output Files</i>	44
4.4	USE ICHANG=3 TO INPUT SOIL STRENGTH BY ELEMENT	44
5.0	LIST OF REFERENCES HTTP://WWW.WUTECGEO.COM/PUBV2D.ASPX FOR VERSAT-2D APPLICATION	45

Appendix A Comparing 1D Soil Column Analyses: SHAKE and VERSAT-1D

Appendix B VERSAT-2D Dynamic Analyses of Upper San Fernando Dam

1.0 INTRODUCTION

VERSAT-2D is a software package consisting of three computer programs, namely, VERSAT-2D Processor (the Processor), VERSAT-S2D and VERSAT-D2D.

It is noted that these three components of VERSAT-2D function independently. Interactions among them take place through data files saved in a Windows Explorer file folder. A brief description for each program is provided below.

VERSAT-2D Processor (the Processor) is a Windows based graphic interface program. It serves as a pre and post processor for VERSAT-S2D and VERSAT-D2D. The program is used to generate a finite element mesh, define soil zones, assign material properties, define boundary conditions, assign pressure loads, and generate input data for VERSAT-S2D & VERSAT-D2D. The program can also display and plot results from analyses such as stresses, displacements, accelerations, pore-water pressures, and a deformed mesh.

VERSAT-S2D is a computer program for static 2D plane-strain finite element analyses of stresses, deformations, and soil-structure interactions. The static analyses can be conducted using stress-strain constitutive relationships from linear elastic model to elasto-plastic models, i.e., Mohr-Coulomb model and Von-Mises model. This program can also be used to compute or determine static pre-existing stresses for use in a subsequent dynamic finite element analysis. Main features of VERSAT-S2D are:

- Linear elastic model
- Von-Mises model for CLAY type
- Mohr-Coulomb model for CLAY, SILT and SAND types
- Stress level dependent stiffness parameters
- External load applications
- Staged construction by adding layers
- Staged excavation by removing layers
- Pore water pressure application
- Calculation of stresses and deformations caused by strain-softening of soils
- Simulation of sheet pile wall and anchors
- Updated Lagrangian analysis
- Factors of safety calculation
- Gravity on and off
- Calculation of pre-existing stresses for use in a dynamic analysis using VERSAT-D2D
- 4-node, 6-node and 8-node solid elements to represent soils



- 2-node line elements to represent sheet pile walls (beam) or anchors (bar/truss)
- Use of any consistent units and sign conventions

VERSAT-D2D is a computer program for dynamic 2D plane-strain finite element analyses of earth structures subjected to dynamic loads from earthquakes, machine vibration, waves or ice actions. The dynamic analyses can be conducted using linear, or nonlinear, or nonlinear effective stress method of analysis. The program can be used to study soil liquefaction, earthquake induced deformation and dynamic soil-structure interaction such as pile-supported bridges. Main features of VERSAT-D2D are:

- Application of horizontal, or horizontal and vertical, ground accelerations at a rigid base
- Application of horizontal outcropping ground velocities at a viscous/elastic base
- Application of a load-time-history at any nodal points
- Global force equilibrium enforced at all time
- Linear elastic model
- Non-linear hyperbolic stress-strain model for SAND type and CLAY type
- Non-linear strain-softening model for SILT type
- Stress level dependent stiffness parameters
- Mohr-Coulomb failure criterion
- **VERSAT-SAND Model** for liquefaction analysis of sandy soils
- **VERSAT-SILT Model** for liquefaction analysis of silty soils (*new since 2016*)
- **Effective Stress Method** of analysis, including the effect of earthquake induced pore water pressure on soil strength and on soil stiffness
- Calculation of ground deformations caused by soil liquefaction
- Calculation of factor of safety against soil liquefaction or strain-softening
- Simulation of sheet pile wall and anchors
- Updated Lagrangian analysis
- Gravity off for **VERSAT-1D module**
- Free-field stress boundary
- 4-node solid elements to represent soils
- 2-node line elements to represent sheet pile walls (beam) or anchors (bar/truss)
- Use of any consistent units and sign conventions
- Probabilistic Seismic Performance Analysis (PSPA) including subduction Interface (e.g., Magnitude 9 or M9) and Non-Interface (e.g., M7) earthquakes (*new since 2018*)
- Local viscous damping (a, b) for stiff structures



FLOW CHART TO ILLUSTRATE TYPICAL STEPS IN A DYNAMIC ANALYSIS:**Step 1:****VERSAT-2D Processor**

- Generate a finite element mesh (2D)
- Define soil zones and material parameters
- Define structural elements and parameters
- Define boundary conditions, apply pressure loads
- Generate input data for VERSAT-S2D or VERSAT-D2D

Step 2:**VERSAT-S2D**

- Conduct static stress analyses
- Conduct static deformation analyses
- Conduct static pore water pressure applications
- Conduct static soil-structure interaction analyses
- Determine pre-existing stresses

Step 3:**VERSAT-D2D**

- Conduct dynamic linear analyses with or without gravity
- Conduct dynamic nonlinear analyses of earth structures subjected to dynamic loads from earthquakes, machine vibration, waves or ice actions
- Conduct dynamic nonlinear effective stresses analyses to determine soil liquefaction (SAND & SILT) and earthquake induced deformations
- Conduct dynamic analyses of soil-structure interaction such as pile-supported bridges

Step 4:**VERSAT-2D Processor**

- View and print finite element mesh including node, element numbers
- View and print soil material zones (Color printer required)
- View and print results of stresses or displacements (peak and instant)
- View and print acceleration values (peak and instant), if applicable
- View and print analysis results of shear strains (peak and instant) or pore water pressure or factor of safety against liquefaction
- View and print deformed mesh
- Save graphics as image files (.emf, or .gif, or .jpeg etc)

2.0 VERSAT-S2D TECHNICAL MANUAL

2.1 Introduction

VERSAT-S2D is a computer program for static 2D plane-strain finite element analyses of stresses, deformations, and soil-structure interactions. The static analyses can be conducted using stress-strain constitutive relationships from linear elastic model to elasto-plastic models, i.e., Mohr-Coulomb model and Von-Mises model. This program can also be used to compute or determine static pre-existing stresses for use in a subsequent dynamic finite element analysis.

2.2 Linear Elastic Model

Elastic materials obey linear elastic stress-strain relationships during loading, unloading, and reloading. From the theory of elasticity for a 2D plane-strain problem, the stress and strain has a linear relationship as follows:

$$[2.1] \quad \{\sigma\} = [D] \{\epsilon\}$$

Where

$\{\sigma\}$ = a stress vector consisting of $\{\sigma_x, \sigma_y, \tau_{xy}\}^T$;

$\{\epsilon\}$ = a strain vector consisting of $\{\epsilon_x, \epsilon_y, \gamma_{xy}\}^T$;

$[D]$ = a matrix of elasticity stiffness defined by shear modulus and bulk modulus of the material.

The shear modulus, G , and the bulk modulus, B , are computed in the program using the following equations:

$$[2.2] \quad G = K_g \bullet P_a$$

$$[2.3] \quad B = K_b \bullet P_a$$

Where

P_a = atmospheric pressure, 101.3 kPa

K_b = bulk modulus constant

K_g = shear modulus constant

The Poisson's ratio, μ , and the Young's modulus, E , can be computed from G and B using:

$$[2.4] \quad \mu = \frac{3B - 2G}{6B + 2G} \quad \& \quad B/G = \frac{2(1 + \mu)}{3(1 - 2\mu)}$$

$$[2.5] \quad E = 2(1 + \mu) \bullet G$$



2.3 Plasticity Strength Models for Soil and Rock

2.3.1 Mohr - Coulomb SAND Model

The Mohr - Coulomb SAND Model is used to simulate material shear strengths that are functions of strength parameters as well as stresses induced by loading. The strength parameters (c' , ϕ' for an effective stress analysis, or c_u , ϕ_u for a total stress analysis) for the model are normally derived from a Mohr – Coulomb stress diagram.

Prior to yield, the stress-strain relationship for the SAND Model is linear elastic. At yield, plastic irrecoverable deformation occurs. The stress-strain relationship is then governed by the theory of plasticity.

For analyses of drained loading conditions (or effective stress analyses of undrained loading conditions¹), the stresses at yield are confined by

$$[2.6] \quad \frac{\sigma_1 - \sigma_3}{2} = c' \cos \phi' + \frac{(\sigma_1 + \sigma_3)}{2} \sin \phi'$$

Where

σ_1, σ_3 = current major and minor principal stresses, respectively;

c', ϕ' = cohesion and friction angle, respectively. These are strength parameters from an effective stress envelope on the Mohr-Coulomb diagram, and they can be measured in consolidated-undrained (CU) tests with pore water pressure measurement or in consolidated-drained (CD) tests.

For analyses of undrained loading conditions, strength parameters c_u and ϕ_u that are derived from a total stress envelope on the Mohr-Coulomb diagram should be used in equation (2.6).

2.3.2 Von - Mises CLAY Model

The Von - Mises CLAY Model is used to simulate material shear strengths that are functions of strength parameters and stresses prior to loading. However, the strengths remain constant during loading. This model can be used to simulate undrained response of low-permeability soils such as clays or silts.

Prior to yield, the stress-strain relationship is linear elastic. At yield, plastic irrecoverable deformation occurs. The stress-strain relationship is then governed by the theory of plasticity. The stresses at yield are confined by:

¹ An effective stress analysis of undrained loading (i.e., saturated sands under earthquake loading) can be conducted in the dynamic analysis using VERSAT-D2D, but the method is not available in static analyses using VERSAT-S2D.

$$[2.7] \frac{1}{\sqrt{6}} \sqrt{(\sigma_1 - \sigma_2)^2 + (\sigma_2 - \sigma_3)^2 + (\sigma_3 - \sigma_1)^2} = S$$

Where

- $\sigma_1, \sigma_2, \sigma_3$ = major, intermediate, and minor principal normal stresses, respectively;
 S = the shear strength of soils prior to loading.

In VERSAT-S2D², the shear strengths (S) of the CLAY Model are computed using one of the following two options:

- Option 1: S is a function of pre-load-application effective normal stresses; and
- Option 2: S is a function of pre-load-application effective vertical stresses.

Option 1: S is computed from

$$[2.8] S = c \cdot \cos \phi + \frac{1}{2} (\sigma_x' + \sigma_y') \sin \phi$$

Where

- σ_x', σ_y' = pre-load-application effective normal stresses in horizontal (X) and vertical (Y) directions, respectively
 c, ϕ = cohesion and friction angle, respectively. For analyses of undrained loading conditions, strength parameters c_u and ϕ_u that are derived from a total stress envelope on the Mohr-Coulomb diagram are normally used herein.

The pre-load-application stresses are stresses just before a load application such as adding a new layer, applying new point loads or changing ground water conditions; and they are updated immediately after completion of this load application. When constructing a multi-layer fill embankment over saturated soft clays, for example, the pre-load-application stresses would be considered as the post-consolidation stresses at completion of consolidation from a previous layer of filling

Option 2: S is computed from

$$[2.9] S = c + k \cdot \sigma_{v_0}'$$

Where

- c, k = shear strength constants that would be derived from results of field vane shear tests or laboratory direct simple shear tests where horizontal stresses are not well defined; and

² The two options are also used in VERSAT-D2D for computing the shear strengths of the CLAY Model.

σ_{vo}' = pre-load-application effective vertical stresses ($=\sigma_y'$).

2.3.3 Shear Strength Models for Silts

Shear strengths for silts are determined either using the Mohr–Coulomb SAND Model or Von-Mises CLAY Model. The following rules are applied for silts:

- Use of parameters c and ϕ : Mohr-Coulomb SAND Model with equation (2.6); or
- Use of parameters c and k : Von-Mises CLAY Model with equations (2.7) and (2.9).

2.4 Stress Level Dependent Stiffness Parameters

When the Mohr-Coulomb SAND Model or the Von-Mises CLAY Model is used, linear elastic shear modulus G and bulk modulus B are considered to be pre-load-application stress dependent:

$$[2.10] \quad G = K_g P_a \left(\frac{\sigma_m'}{P_a} \right)^m$$

$$[2.11] \quad B = K_b P_a \left(\frac{\sigma_m'}{P_a} \right)^n$$

Where

P_a = atmospheric pressure, e.g., 101.3 kPa

K_b = bulk modulus constant

K_g = shear modulus constant

m, n = shear modulus exponential, and bulk modulus exponential, respectively

σ_m' = pre-load-application effective mean normal stress, and

$$[2.12] \quad \sigma_m' = \frac{1}{3}(\sigma_x' + \sigma_y' + \sigma_z')$$

2.5 Bending Elements for Structural Members

Beam elements are used to model the bending behavior of structural members such as beams, sheet piles or tunnel walls. The bending stiffness of a beam element is given by

$$[2.13] \quad [K] = \frac{EI}{L^3} \begin{bmatrix} 12 & 6L & -12 & 6L \\ 6L & 4L^2 & -6L & 2L^2 \\ -12 & -6L & 12 & -6L \\ 6L & 2L^2 & -6L & 4L^2 \end{bmatrix}$$

Where

E = Young's modulus of the structural member (the beam), and $E = K_E * P_a$;



I = the bending moment of inertia of the beam per unit width³;

L = length of the beam element.

The axial stiffness of the beam element is given by

$$[2.14] \quad K_A = R_b \frac{EA}{L}$$

Where:

A = sectional area of the beam

R_b = a reduction factor used to reduce the axial stiffness of the beam. The use of a R_b value from 0 to 1 can simulate a variable degree of frictions between the structural members and the surrounding soils.

The beam elements can be used to simulate approximately the bending behavior of one row or multiple rows of piles distributed in the direction perpendicular to the 2D XOY plane. However, adjustments in structural properties would be needed since the piles, except a wall of sheet piles, do not form a continuous pile-wall in the direction perpendicular to the 2D XOY plane .

Beam elements can be orientated in any direction within the 2D XOY plane.

2.6 Spring Elements for Structural Members

Linear elastic spring elements (truss/bar) can be used to model anchors, struts or shoring supports. The axial stiffness of a spring (truss/bar) element is defined by

$$[2.15] \quad K_A = \frac{EA}{L}$$

Where

E = Young's modulus of the structural members (the truss), and $E = K_E * P_a$;

A = sectional area of the truss;

L = the length of the truss element.

Appropriate adjustments in structural properties would be needed when truss elements are used to model structural members, such as struts, that are not continuous in the direction perpendicular to the 2D XOY plane.

³ For example, $I=1/12*bh^3$ is for a rectangular section with a width of b and a height of h ; and $I=1/64\pi* d^4$ (where $\pi=3.1416$) is correct for a circular section having a diameter of d . However, they would require some adjustments in a 2D plane-strain application ($I_{2D}=I_{pile}/s$ and $M_{pile} = M_{2D} * s$, where s represents the spacing of piles in the 3rd direction and M represents bending moment).

The truss elements can be orientated in any direction within the 2D XOY plane.

2.7 Pore Water Pressure and Effective Stresses

In static analyses using VERSAT-S2D, pore water pressures induced by loading in a load application are not considered. Instead, hydrostatic or steady state pore water pressures are assigned to soil elements using the following two methods:

- Method 1⁴: An element is assigned to a water table or a phreatic surface.
- Method 2: An element is assigned to a non-zero pore water pressure value (e.g., from a piezometric line) or pore water pressure ratio, r_{u0} ;

The following rules are applied when using the above two methods:

- Pore water pressure in an element is first calculated by the program using Method 1. Any element that is located below the water table is assigned a pore-water pressure value equal to the hydrostatic water pressure at the element center calculated using the net pressure head in the vertical direction;
- The pore water pressure in an element determined using Method 2, if it is not zero, would replace the value calculated using Method 1, i.e., Method 2 take precedence to Method 1.

Therefore, Method 1 and Method 2 could be applied simultaneously to different zones of a finite element model to simulate various static pore water pressure conditions. But, pore water pressures determined using Method 2 can't be changed (i.e., constant) during a static analysis although the static analysis can contain several static runs, and each static run could consist of a few load applications. However, a multi-run static analysis can have several water tables because each static run can define its own water table. For example, Method 1 can be used to simulate rising water tables in dams during initial reservoir water filling.

When r_{u0} is specified, the pore water pressure in an element is computed by

$$[2.16] \quad u_0 = r_{u0} \cdot \sigma_{v0}'$$

Where

u_0 = static pore water pressure;

σ_{v0}' = pre-existing⁵ effective vertical stress at the element center; and

⁴ When the Option $ywt0 > 0$ is invoked in a large-strain static analysis or in a dynamic analysis, Method 1 (i.e., a water table) must be used to define the existing (or static) pore water pressures in the entire model; see User's Manual Section 2.7 for further details. The use of $ywt0$ Option will erase all existing PWP assigned using Method 2.

⁵ . In VERSAT-2D static and dynamic analyses, pre-existing stresses are always obtained from an input file with an extension of PRX, which contains model stresses computed from a previous static analysis and saved (in an output file with an extension of PR4) for a subsequent static analysis or for a dynamic analysis. The PR4 file is then renamed as PRX file.



r_{u0} = static pore water pressure ratio.

Effective Stresses: The normal stresses used in static analysis of VERSAT-S2D are effective stresses (σ') calculated to be the total stresses (σ) subtracted by pore water pressures (u_0) determined using Method 1 or Method 2 above, i.e., $\sigma' = \sigma - u_0$.

2.8 Calculation of Stresses and Deformations Caused by Strain-Softening of Soils

When the Mohr-Coulomb SAND Model or the Von-Mises CLAY Model is used, the program checks the state of current stresses against the corresponding yield condition. Compatibility between stresses and the yield condition is always maintained throughout the analysis. Soil strengths may change in the event of loading or straining. For instance, shear strengths of sandy soils will likely reduce when dynamic pore water pressures develop under earthquake loading.

The program can be used to compute stresses and deformations caused by strain-softening of soils. This is done by assigning a new set of soil parameters, such as reduced shear strengths.

2.9 Updated Lagrangian Analysis

The geometry of a mesh is continuously updated during the calculation when the updated Lagrangian analysis is chosen. This option is provided for solving problems involving large strain deformations.

2.10 Factors of Safety

Factor of safety, f_{os} , against shear failure is calculated by the program for each soil element using the following equation:

$$[2.17] \quad f_{os} = \frac{S}{\tau_{\max}}$$

Where

τ_{\max} = maximum shear stress in the element; and

$$[2.18] \quad \tau_{\max} = \sqrt{\frac{1}{4}(\sigma_y - \sigma_x)^2 + \tau_{xy}^2}$$

Where

σ_x, σ_y = normal stresses in horizontal (X) and vertical (Y) directions, respectively;

τ_{xy} = current shear stress in the XoY plane.

S = shear strength. For CLAY Model, S is defined in equation (2.7); for SAND Model, S is equal to the right-hand side of equation (2.6), i.e.

$$[2.19] \quad S = c' \bullet \cos \phi' + \frac{(\sigma_1 + \sigma_3)}{2} \sin \phi'$$

2.11 Gravity On and Off

Normally gravity force is always acting downward in the model. In the absence of external nodal loads, force equilibrium is maintained between gravity force and internal force consisting of soil effective stresses and pore water pressures. Gravity force can be set off for analyses of structures not involving gravity.

2.12 Units and Signs

The program accepts any consistent units. The two more commonly used unit systems are metric units and imperial units. In metric units, the length is expressed in meter, acceleration in m/s^2 , and pressure in kilopascal (kPa). In imperial unit, the length is expressed in feet, acceleration in ft/s^2 , and pressure in pound (lb) per square feet (psf). Examples of consistent units are shown in the following table.

Property	Units	Metric	Imperial
Geometry	L	metres	feet
Water Unit Weight	F/L ³	kN/m ³	pcf
Soil Unit Weight	F/L ³	kN/m ³	pcf
Cohesion	F/L ²	kPa	pcf
Pressure	F/L ²	kPa	psf
Force F	kN	lb	
E (modulus)	F/L ²	kPa	psf

The gravity acceleration, unit weight of water and the atmospheric pressure must be entered correctly for whichever system of units you may have chosen. These parameters are used throughout the analysis.

In the program, tensile stress is considered positive; compressive stress is negative. Pore water pressure is considered positive.



3.0 VERSAT-D2D TECHNICAL MANUAL

VERSAT-D2D is a computer program for dynamic 2D plane-strain finite element analyses of earth structures subjected to dynamic loads from earthquakes, machine vibration, waves or ice actions. The dynamic analyses can be conducted using linear, or nonlinear, or nonlinear effective stress method of analysis. The program can be used to study soil liquefaction, earthquake induced deformation and dynamic soil-structure interaction such as pile-supported bridges (Wu, 2001; Wu et al., 2006; Wu, 2010; BC Hydro 2010, 2012, 2013; Finn and Wu, 2013; Sweeney and Yan, 2014; Wu, 2015)

3.1 System Equations of Motions and Modal Frequencies

3.1.1 Equations of Motions

For the case of base acceleration input, displacements relative to the base are computed. Therefore, the relative displacements at the base are zero. Inertial forces on the soil mass caused by base motions are computed using the Newton's law, and base accelerations are used directly in the equations of motions. The equations describing the incremental dynamic force equilibrium are given as

$$[3.1] \quad [M]\{\Delta \frac{d^2\delta}{dt^2}\} + [C]\{\Delta \frac{d\delta}{dt}\} + [K]\{\Delta\delta\} = \{\Delta P\}$$

Where

[M] = mass matrices

[C] = viscous damping matrices

[K] = tangent stiffness matrices

[$\Delta\delta$] = incremental displacement matrices

[$\Delta d\delta/dt$] = incremental velocity matrices

[$\Delta d^2\delta/dt^2$] = incremental acceleration matrices

[ΔP] = incremental external load matrices

3.1.2 Modal Frequencies and Periods

The nonlinear dynamic analyses are conducted using the finite element method in the time domain; this method allows that eigenvalues and modal angular frequencies, $\omega_1, \omega_2, \omega_3, \omega_4, \omega_5$, and so on, of the entire system be computed at the time interval (specified by the user, e.g., 1.5 sec used in Figure 1a for the example) using the following system equation:

$$[K] - \omega^2[M] = 0$$

Where

[M] is mass matrix of the entire system, as in Eq. [3.1] and it is constant with time;

[K] is the stiffness matrix of the entire system, but it varies with time as the soil modulus of each soil element varies with time and with the level of shaking intensity.

The fundamental period (1st mode) of a structure (such as an earthfill dam) and its variation during the duration of shaking (see Figure 1a) are often required in order to develop appropriate ground motion records for dynamic time history analysis of the structure.

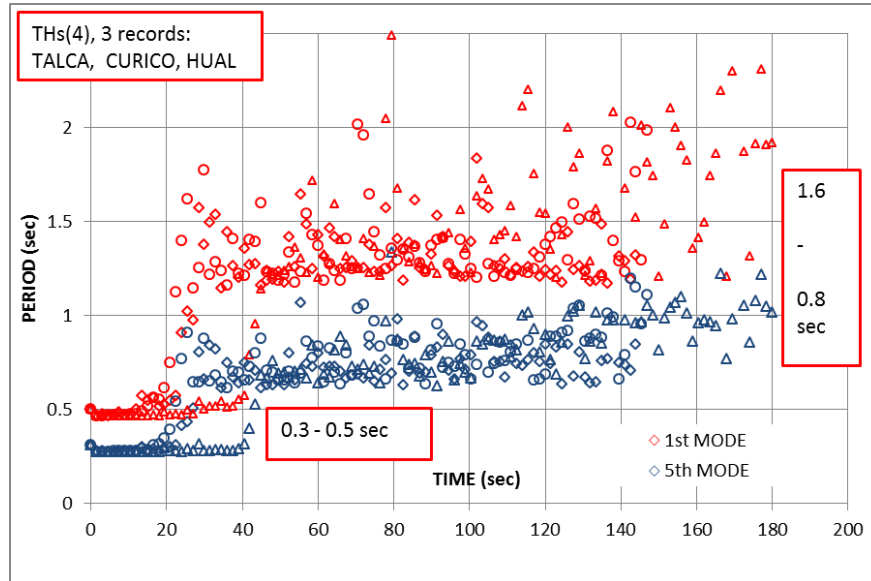


Figure 1a Variations of 1st and the 5th Modal Periods, computed by VERSAT-2D, with time of shaking for three ground motion records from the Chile Maule M8.8 Subduction Earthquakes

3.2 Viscous Damping

3.2.1 System Damping for Global Structure

In a linear elastic analysis, system damping consists only of viscous damping. In the analysis, viscous damping is assumed to be Rayleigh type and thus is computed by

$$[3.2] \quad [C] = a[M] + b[K]$$

Where

$$[3.3] \quad a = 2\lambda_m \omega_1$$

$$[3.4] \quad b = 2\lambda_k / \omega_1$$

The total damping at the first mode, i.e. ω_1 is

$$[3.5] \quad \lambda = \lambda_m + \lambda_k = \frac{b \omega_1}{2} + \frac{a}{2\omega_1}$$

Where



λ_m = the mass proportional Raleigh damping (%) at first mode

λ_k = the stiffness proportional Raleigh damping (%) at first mode

3.2.2 Viscous Damping for Local Structure

Since Version 2019.10.3, the program allows viscous damping [C] be calculated for specified local materials, such as for concrete structures or steel sheet piles that have much higher natural frequencies than the soils. This is accomplished by assigning material-related viscous damping constants (a & b) in Eqs. [3.3] and [3.4] based on the modal frequency ω_1 of the local structures of interest.

3.3 Linear Elastic Model

Elastic materials obey linear elastic stress-strain relationships during loading, unloading, and reloading. From the theory of elasticity for a 2D plane-strain problem, the stress and strain has a linear relationship as follows:

$$[3.6] \quad \{\sigma\} = [D] \{\epsilon\}$$

Where

$\{\sigma\}$ = a stress vector consisting of $\{\sigma_x, \sigma_y, \tau_{xy}\}^T$;

$\{\epsilon\}$ = a strain vector consisting of $\{\epsilon_x, \epsilon_y, \gamma_{xy}\}^T$, where

$$\epsilon_x = d\delta_x/dx; \quad \epsilon_y = d\delta_y/dy; \quad \gamma_{xy} = d\delta_x/dy + d\delta_y/dx$$

[D] = a matrix of elasticity stiffness defined by shear modulus and bulk modulus of the material.

The shear modulus, G, and the bulk modulus, B, are computed in the program using the following equations:

$$[3.7] \quad G = K_g \bullet P_a$$

$$[3.8] \quad B = K_b \bullet P_a$$

Where

P_a = atmospheric pressure, 101.3 kPa

K_b = bulk modulus constant

K_g = shear modulus constant



3.4 Nonlinear Hyperbolic Stress - Strain Model

3.4.1 Low - Strain Stiffness Parameters

When the nonlinear hyperbolic stress – strain model is used, the low - strain shear modulus, G_{\max} , and the bulk modulus, B , are pre-existing stress level dependent and are computed as follows:

$$[3.9] \quad G_{\max} = K_g P_a \left(\frac{\sigma_m'}{P_a} \right)^m$$

$$[3.10] \quad B = K_b P_a \left(\frac{\sigma_m'}{P_a} \right)^n$$

Where

P_a = atmospheric pressure, 101.3 kPa

K_b = bulk modulus constant

K_g = shear modulus constant

m, n = shear modulus exponential, and bulk modulus exponential, respectively

σ_m' = pre-existing effective mean normal stress from the static analysis

$$[3.11] \quad \sigma_m' = \frac{1}{3} (\sigma_x' + \sigma_y' + \sigma_z')$$

It is noted that G_{\max} is also called the initial shear modulus of the hyperbolic stress – strain model; and it is quite different from the elastic shear modulus G in equations (2-10) which represents the secant shear modulus over the range of shear strains caused by static loading.

3.4.2 Hyperbolic Shear Stress-Strain Model

The relationship between shear stress, τ_{xy} , and shear strain, γ , for an initial loading condition is assumed to be nonlinear and hyperbolic (Figure 1b) as follows:

$$[3.12] \quad \tau_{xy} = \frac{G_{\max} \gamma}{1 + G_{\max} / \tau_{ult} \bullet |\gamma|}$$

Where

τ_{ult} = ultimate shear stress in the hyperbolic model;

G_{\max} = low-strain shear modulus; and $G_{\max} = \rho V_s^2$ with ρ being the soil density and V_s being the shear wave velocity.

The Masing criterion has been used to simulate the shear stress-strain relationship during unloading and reloading. A detailed description about this non-linear stress-strain model can be

found in Finn et al. (1977). The extended application of Masing criterion to irregular loading such as earthquake loading was also presented by Finn et al. (1977).

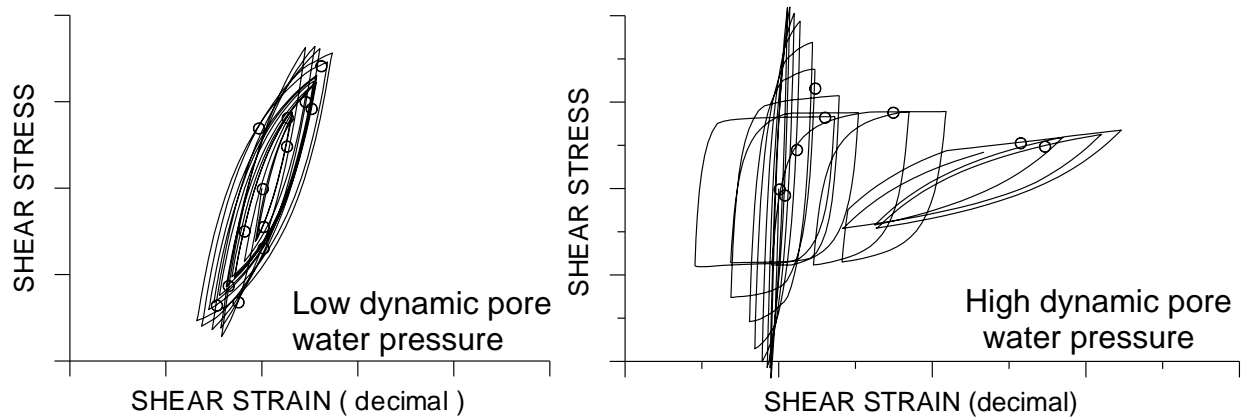


Figure 1b Typical hyperbolic shear stress-strain histories showing hysteresis loops

3.4.3 Determination of Ultimate Shear Stress

The ultimate shear stress in equation [3.12] is determined using one of the following two options:

- Option 1: τ_{ult} is the shear strength at start of dynamic loading; or
- Option 2: τ_{ult} is proportional to the initial shear modulus G_{max} .

Option 1: τ_{ult} is taken as τ_f

$$[3.13] \quad \tau_{ult} = \tau_f$$

Where

τ_f = shear strength at start of dynamic loading. The equations presented in Section 3.7 for computing shear strengths for SAND Model and CLAY Model are applied with pre-existing normal stresses being used in these equations.

Option 2: τ_{ult} is computed from

$$[3.14] \quad \tau_{ult} = \frac{G_{max}}{R_f}$$

Where

R_f = a modulus reduction factor.

Input of a non-zero value of R_f for a material number triggers the use of equation [3.14], instead of equation [3.13], for computing the ultimate shear stresses for soil elements having this material number, unless τ_{ult} computed from equation [3.14] is less than from equation [3.13]. The use of equation [3.14] attempts to match a reduction curve of shear

modulus versus shear strain at a strain range of interest by selecting an appropriate value of R_f (Figure 2).

In a total-stress nonlinear analysis, the ultimate shear stresses computed using the above described procedures are used directly and their values remain unchanged, for SAND Model or CLAY Model, during dynamic loading. However, in an effective stress nonlinear analysis, the effect of dynamic pore water pressure on soil stiffness, i.e. initial shear modulus and ultimate shear stresses, is also considered for the SAND Model (see Section 3.6.3).

3.4.4 Hysteretic Damping in a Hyperbolic Model

In a nonlinear analysis, the hysteretic damping is inherently included by following the nonlinear hysteresis loop of shear stress-strain response. The Masing criterion used in the hyperbolic model during unloading and reloading provides hysteretic damping as shown in Figure 2.

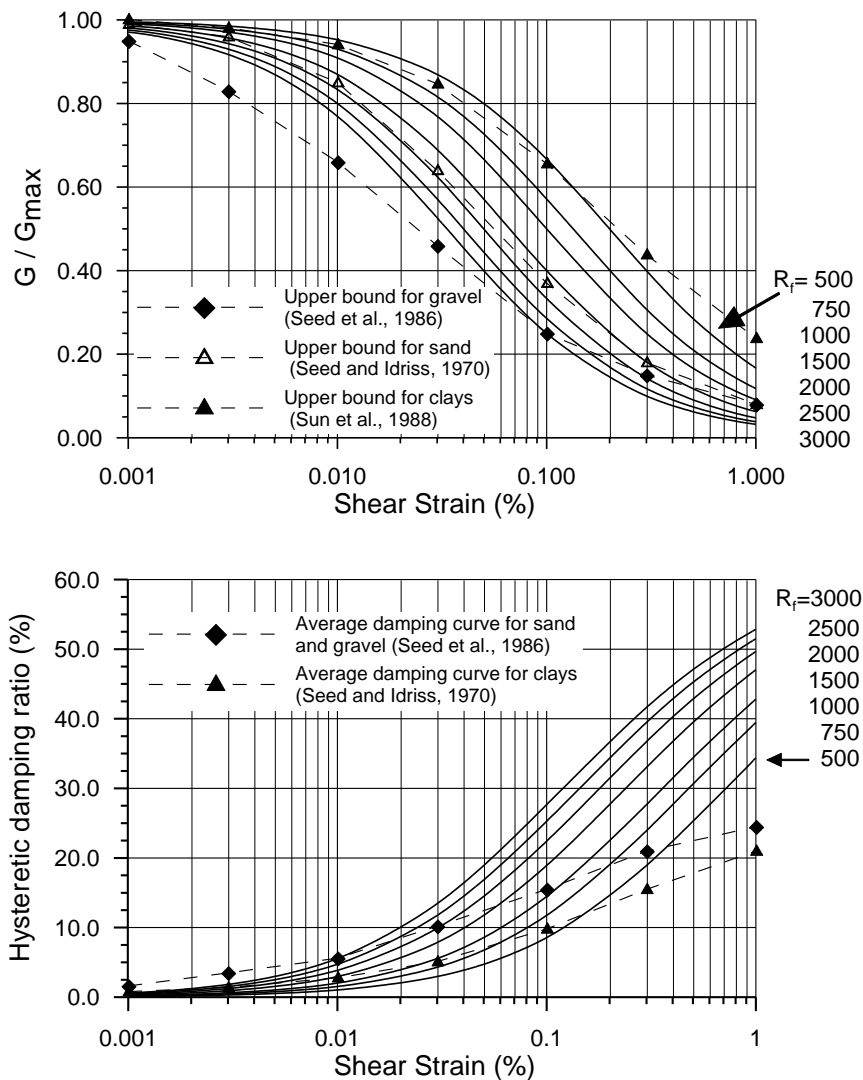


Figure 2 Secant shear modulus and damping ratios for various values of R_f in a hyperbolic stress – strain model (after Wu, 2001)



During a nonlinear analysis, the viscous damping, which is also of Rayleigh type as in a linear analysis, is used to control any high frequency oscillations in response that may arise from numerical integration.

3.5 SAND Model - Dynamic Pore Water Pressure Models

In a Non-linear Effective Stress analysis using VERSTA-2D, the PWP and the effective stresses (and associated effective shear strengths) in soil elements are updated with time regardless of which PWP models being adopted.

Once liquefaction is triggered the post-liquefaction residual strength (undrained strength, explicit parameters input by the user) of the soil is applied and kept constant from the time of triggering.

3.5.1 Introduction

An effective stress analysis takes into account the effect of dynamic pore water pressures on dynamic response of sands or silts. The following rules are applied regarding generation of dynamic pore water pressures:

- SAND Model can develop dynamic pore water pressure;
- CLAY Model would not develop dynamic pore water pressures.

Dynamic pore water pressures are caused by plastic deformations in the sand skeleton and persist until dissipated by drainage or diffusion. They have a great impact on the strength and stiffness of the sandy soils and should be taken into account in the analysis.

The dynamic pore water pressures modelled by the program will show a steady accumulation of pressure with time but will not show a fluctuation of pressure caused by a change in transient mean normal stress. The transient pressures are balanced by the mean normal stresses and have little effect on stability and deformability of soils. Therefore the transient pore water pressures are not modelled in the analysis.

The increments in pore water pressure Δu that develop in saturated soils under seismic shear strains are related to the plastic volumetric strain increments, $\Delta \epsilon_v^p$, that occur in the same soil under drained conditions with the same shear strain history. For saturated sandy soils in an undrained condition, water may be assumed to be effectively incompressible compared to the soil skeleton. Thus under a condition of zero-volume change, Martin et al. (1975) proposed the following relationship for computing the dynamic pore water pressure increment Δu

$$[3.15] \quad \Delta u = E_r \bullet \Delta \epsilon_v^p$$

Where

$\Delta \epsilon_v^p$ = Plastic volumetric strain increment accumulated during a period of strain history

- Δu = Dynamic pore water pressure increment corresponding to the plastic volumetric strain increment $\Delta \varepsilon_v^p$
- E_r = Rebound modulus of the soil skeleton corresponding to the current effective vertical stress.

Three models are available for computing dynamic pore water pressures in sands and silts. The first model was developed by Martin-Finn-Seed (MFS) in 1975. The second model is a modification of the MFS model proposed by Wu (1996). These two models calculate the dynamic pore water pressures using the rebound modulus and the plastic volumetric strain, i.e., using equation [3.15]. The third model was developed by Seed et al. (1976) who determined the dynamic pore water pressures based on the number of cyclic shear stresses.

3.5.2 Plastic Volumetric Strain

Under a drained simple shear condition, the volumetric strain increment $\Delta \varepsilon_v^p$ is a function of the total accumulated volumetric strain ε_v^p and the amplitude of the current shear strain γ . Byrne (1991) modified the original MFS model (Martin et al., 1975) and proposed the following 2-parameter relationship:

$$[3.16] \quad \Delta \varepsilon_v^p = C_1 \gamma \cdot \text{Exp}\left(-C_2 \frac{\varepsilon_v^p}{\gamma}\right)$$

The volumetric strain constants, C_1 and C_2 , depend on the sand type and relative density of the sand. In practice these constants may be estimated using the relationships proposed by Byrne (1991)

$$[3.17] \quad C_1 = 8.7(N_1)_{60}^{-1.25}$$

$$[3.18] \quad C_2 = \frac{0.4}{C_1}$$

Where

$(N_1)_{60}$ = Standard Penetration Test (SPT) N values normalized to 60% standard hammer energy and an overburden stress of approximately 100 kPa.

Under harmonic loads, the plastic volumetric strain increment, $\Delta \varepsilon_v^p$, is usually accumulated at each cycle or at each half cycle of strain. Under irregular earthquake loads, $\Delta \varepsilon_v^p$ may be accumulated at points of strain reversal.

3.5.3 Martin-Finn-Seed's Pore Water Pressure Model

In the Martin-Finn-Seed (MFS) model, an analytical expression for the rebound modulus E_r , at any effective stress level σ_v' , is given by Martin et al. (1975) as

$$[3.19] \quad E_r = \frac{(\sigma_v')^{1-m}}{mK_2(\sigma_{v0}')^{n-m}}$$

Where

σ_{v0}' = initial value of the effective stress

K_2 , m , n = experimental constants derived from rebound tests ($m=0.43$ & $n=0.62$ are used in the program)

3.5.4 Modified MFS Pore Water Pressure Model

Wu (1996, 2001) proposed that the rebound modulus, E_r , be determined using the current effective vertical stress σ_v' as

$$[3.20] \quad E_r = M \cdot \sigma_v'$$

Or

$$[3.21] \quad E_r = M \cdot (\sigma_{v0}' - u)$$

Where

M = rebound modulus constant

σ_{v0}' = initial effective vertical stress

u = current dynamic pore water pressure

Determination of rebound modulus number is based on the volume-constant concept that there is a unique relationship between the relative density of sand and the amount of potential volumetric strain required to trigger initial liquefaction. Ishihara and Yoshimine(1992) stated that " the volume change characteristics of sand during re-consolidation following the cyclic loading is uniquely correlated with the amount of developed pore water pressure, no matter what types of irregular loads are used, and irrespective of whether the irregular load is applied in one-direction or in multi-directional manner." Their work strongly supports that at a specific relative density the sample will experience initial liquefaction if a certain amount of potential volumetric strain (referred as volume change during re-consolidation following the cyclic loading by Ishihara and Yoshimine) is developed in the sample.

Relationships between pore water pressure ratio and plastic volumetric strain for various values of M are presented in Figures 3a and 3b. The constant-volume pore water pressure model, or the modified MFS model, has been verified by Wu (1996) using test data by Bhatia (1980). The computed pore water pressure response agrees well with the experimental response for sample of $D_r = 45\%$ to 60% .

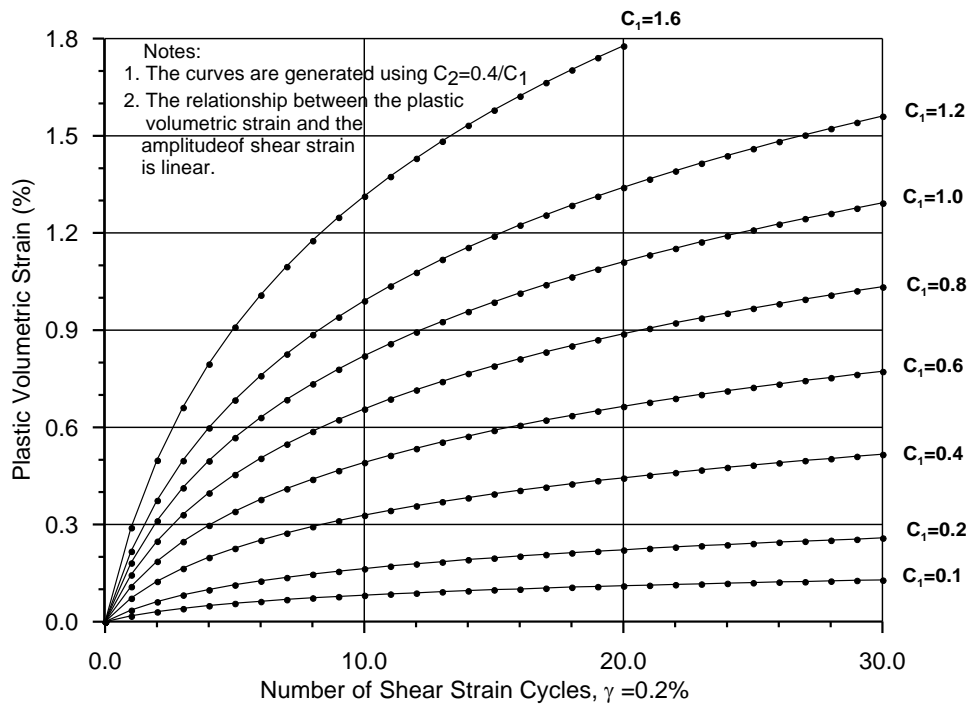


Figure 3a Relationship between plastic volumetric strain and number of shear strain cycles in the MFS pore water pressure model (after Wu, 1996, 2001)

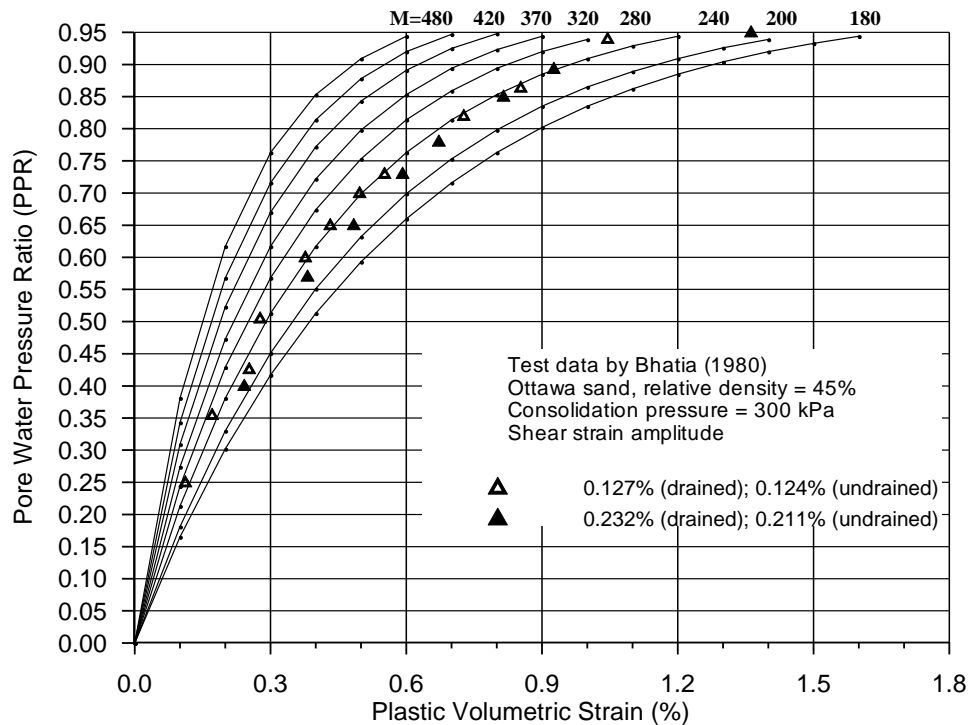


Figure 3b Relationship between pore water pressure ratio (PPR) and plastic volumetric strain in the modified MFS pore water pressure model (after Wu, 1996, 2001)



3.5.5 Seed's Pore Water Pressure Model

Seed et al. (1976) proposed the following relationship (Figure 4)

$$[3.22] \quad u / \sigma_{v0}' = \frac{2}{\pi} \arcsin \left(\frac{N_{15}}{N_1} \right)^{\frac{1}{2\theta}}$$

where θ is an empirical constant; N_1 is the number of uniform shear stress cycles which cause liquefaction⁶; and N_{15} is the equivalent number of uniform shear stress cycles, and

$$[3.23] \quad N_{15} = \sum N_{15(1)}$$

The following equation is used to convert shear stresses of irregular amplitudes to uniform shear stress cycles (Wu, 2001):

$$[3.24] \quad N_{15(1)} = \left(\frac{\tau_{cyc}}{\tau_{15}} \right)^\alpha$$

where τ_{15} is the shear stress required to cause liquefaction in 15 cycles;

τ_{cyc} is cyclic shear stress of any amplitude;

$N_{15(1)}$ is the equivalent number of cycles corresponding to τ_{15} for 1 cycle of τ_{cyc} ; and

α is a shear stress conversion constant.

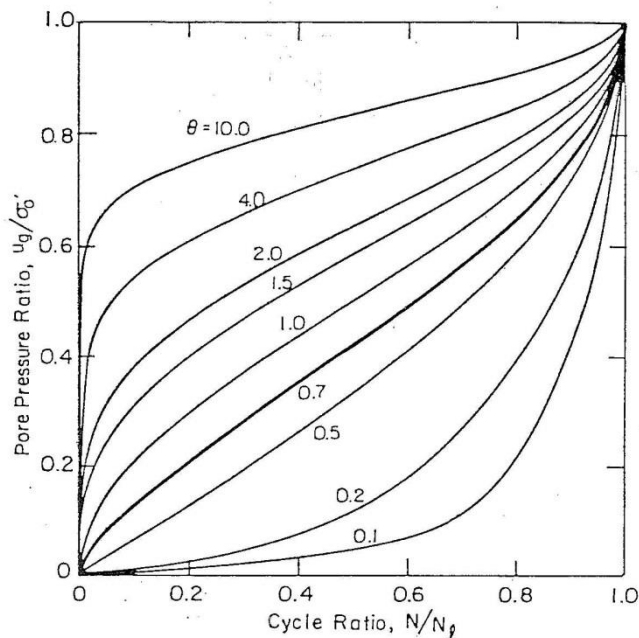


Figure 4 Pore water pressure ratios versus cycle ratios (after Seed et al., 1976)

⁶ For an earthquake magnitude of 7.5, N_1 of 15 is used by the program.

According to Wu (2001), the following two equations are used to relate the number of cycles to cause initial liquefaction at τ_{cyc} , N_{cyc} , the magnitude correction factor, K_M , and the number of representative cycles corresponding to earthquake magnitude, N_M , as shown in Figure 5.

$$[3.25] \quad \frac{\tau_{cyc}}{\tau_{15}} = \left(\frac{15}{N_{cyc}} \right)^{\frac{1}{\alpha}}$$

$$[3.26] \quad K_M = \left(\frac{15}{N_M} \right)^{\frac{1}{\alpha}}$$

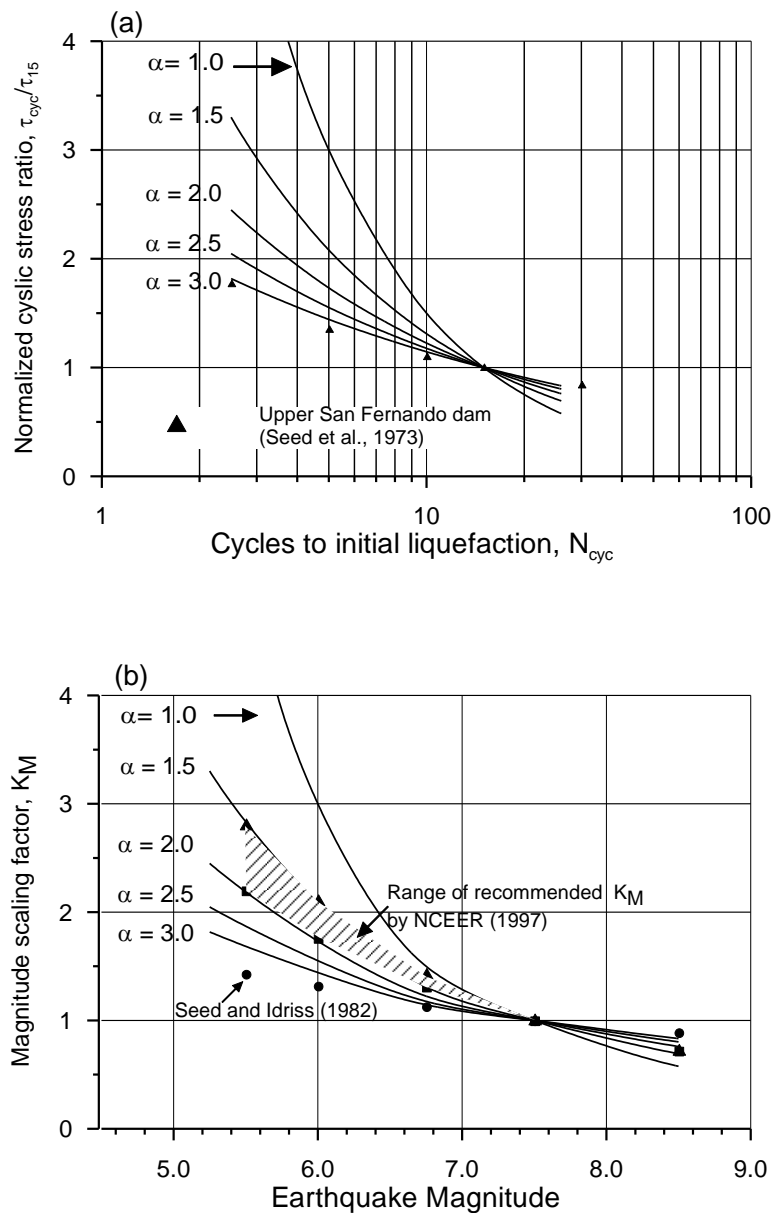


Figure 5. (a) Normalized cyclic stress ratios. (b) Magnitude scaling factors for various values of α in equation (3.24) (after Wu, 2001)



The shear stress ratio to cause liquefaction in 15 cycles for an individual soil element at its own vertical and shear stresses, CRR_{15} (or τ_{15}), is calculated using the following equation:

$$[3.27] \quad crr_{15} = CRR_{15} \cdot K_{\sigma} \cdot K_{\alpha} \quad \text{or,} \quad \tau_{15} = (CRR_{15} \cdot K_{\sigma} \cdot K_{\alpha}) \sigma'_{v0}$$

Where the overburden stress correction, K_{σ} , is made by the β factor using:

$$[3.28] \quad K_{\sigma} = (P_a / \sigma'_{v0})^{\beta}$$

No lower limit is applied to K_{σ} ; but K_{σ} is set by the program to 1.0 if $K_{\sigma} > 1.0$ is calculated from the equation. For example, $\beta \approx 0.25$ could be input according to Youd et al. (2001) for K_{σ} .

SPT blow counts corrected for overburden stress and hammer energy, $(N_1)_{60}$, can be used for determining the cyclic resistance ratio, CRR_{15} , for sands (clean or with fines) at an effective vertical stress of $\sigma'_{v0} = 1$ tsf (i.e., about 101.3 kPa) using the modified Seed's curve (Figure 6) recommended in Youd et al. (2001).

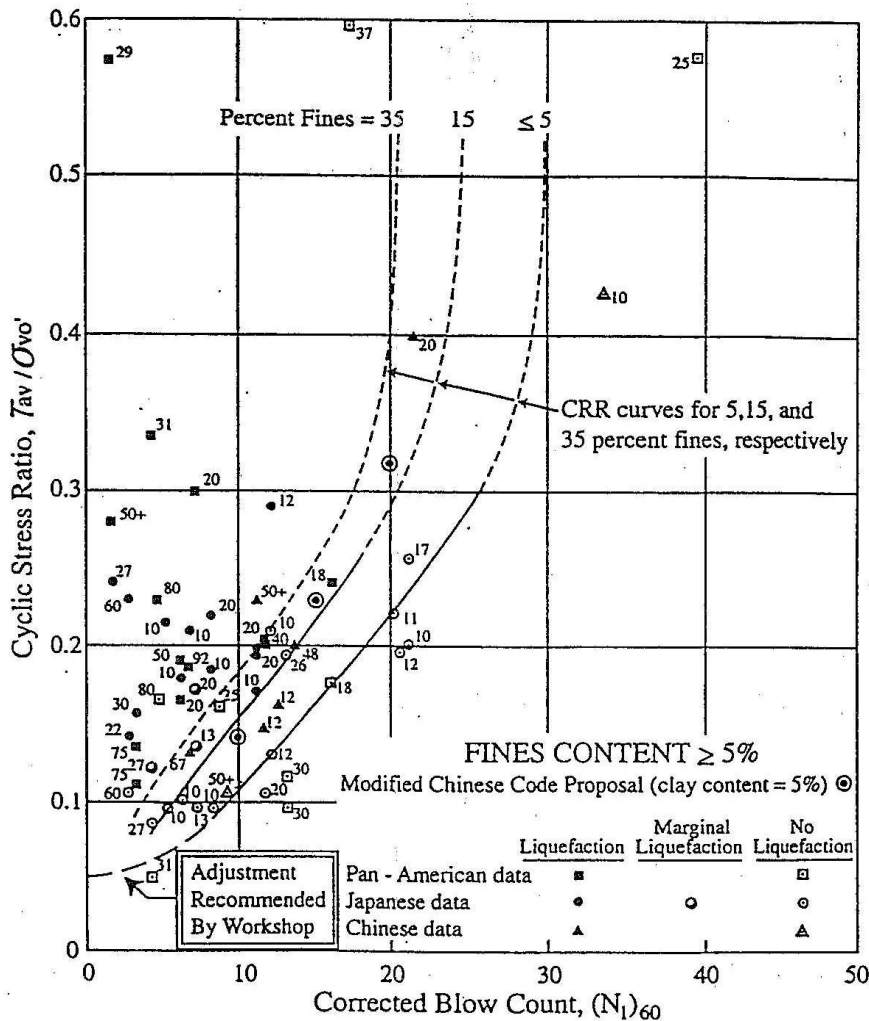


Figure 6 Relationships between cyclic resistance ratio, CRR_{15} at $\sigma'_{v0}=1$ tsf, and corrected SPT blow counts, $(N_1)_{60}$, normalized to approximately 100 kPa (after Youd et al., 2001)



When $(N_1)_{60}$ is selected as input by the user, then the program computes $CRR_{15} = \text{Max} [0.05, 0.011 * (N_1)_{60}]$ for $(N_1)_{60} < 25$, and $CRR_{15} = 0.275 + 0.045 * [(N_1)_{60} - 25]$ for $(N_1)_{60} \geq 25$. For example, CRR_{15} is calculated by the program to be 0.22 for $(N_1)_{60} = 20$.

For other cases, when $(N_1)_{60}$ is not available or the above equations are not applicable, CRR_{15} can be specified by user as input, such as based on laboratory test results.

The effect of static shear stress on cyclic resistance, K_α factor, is not directly taken into account in the calculation of τ_{15} in equation [3.27], i.e., $K_\alpha=1.0$ is used. However, the K_α effect could be included by increasing ($K_\alpha>1.0$) or decreasing ($K_\alpha<1.0$) of CRR in equation [3.27] for zones with known K_α . Laboratory cyclic tests on sands appear to indicate that K_α could be either greater or less than 1.0, depending on details of sands used in testing.

3.6 Effective Stress Dynamic Analysis

The effective stresses used in static analysis of VERSAT-S2D (see Section 2.7) include reduction of total normal stresses (σ) by static pore water pressures, u_0 . The same concept of effective stress still applies in dynamic analysis of VERSAT-D2D.

In addition, in an effective stress dynamic analysis, the effective stress (σ') is further reduced by dynamic pore water pressures (u), i.e., $\sigma' = \sigma - u_0 - u$.

A dynamic effective stress analysis is conducted to accomplish the following tasks:

1. Compute dynamic pore water pressures (u);
2. Compute factors of safety against soil liquefaction or dynamic pore water pressure ratio;
3. Compute effective stresses (σ'), and use σ' and pore water pressures (u_0 & u) in dynamic force equilibrium;
4. Reduce soil stiffness and shear strength based on u ;
5. Determine triggering of soil liquefaction based on u ;
6. Apply post-liquefaction stiffness and shear strength to liquefied soils;
7. Compute ground displacements from cyclic volume change or consolidation of u .

When a total stress nonlinear dynamic analysis is chosen and conducted, the program would carry out calculations for steps 1 and 2 above and output the results; but it would not carry out steps 3 to 7.

An effective stress analysis would have no impact to response of CLAY Model as the CLAY Model does not generate dynamic pore water pressure.

3.6.1 Factors of Safety against Soil Liquefaction

Factor of safety against soil liquefaction is calculated and reported in output by the program if Seed's pore water pressure model is used for the calculation of dynamic pore water pressures. The factor of safety against liquefaction is defined by (Seed and Harder, 1990; Youd et al., 2001):

$$[3.29] \quad FS_{liq} = \frac{\tau_{15}}{\tau_{cyc}}$$

Using N_{15} and α as defined in equations [3.23] and [3.24], the factor of safety can be further calculated using the following equation:

$$[3.30] \quad FS_{liq} = \left(\frac{15}{N_{15}}\right)^{\frac{1}{\alpha}}$$

VERSAT-2D dynamic analysis is always for undrained condition (i.e., PWP does not dissipate during shaking), and thus FS_{liq} always decreases during shaking. However, the program can stop generating PWP at a time specified by the user. FS_{liq} is calculated for each individual soil element and it is the lowest at the end of shaking. FS_{liq} is tracked and saved for result presentation only (not used in analysis), but the equivalent PWP is actually used by the program in the analysis.

3.6.2 Dynamic Pore Water Pressure Ratio: r_u

Dynamic pore water pressure ratio, r_u (or *ppr*), is calculated and reported in output (*.OUD) by the program when the MFS pore water pressure model or the modified MFS pore water pressure model is used. In time history results, r_u is always saved for all three pore water pressure models (Figure 7), including Seed's model. The r_u is defined by:

$$[3.31] \quad ru = \frac{u}{\sigma_{v0}'}$$

u = dynamic pore water pressure caused by earthquake loading;

r_u = dynamic pore water pressure ratio ($ppr = r_u$); liquefaction is triggered when $r_u \geq 0.95$.

3.6.3 Reduction of Stiffness by Dynamic Pore Water Pressure

In an effective stress analysis, the effect of u on soil stiffness is considered by reducing the initial shear modulus and ultimate shear stress (Figure 7) as follows:

$$[3.32] \quad G_0 = G_{\max} \sqrt{\frac{\sigma_v'}{\sigma_{v0}'}}$$

$$[3.33] \quad \tau_0 = \tau_{ult} \frac{\sigma_v'}{\sigma_{v0}'}$$

Where

G_0 = the updated initial shear modulus for the hyperbolic model;

τ_0 = the updated ultimate shear stress for the hyperbolic model.

The program would ensure that G_0 and τ_0 are limited (i.e., not less than) by the respective values of post-liquefaction shear modulus and shear strength of the same soil. In addition, τ_0 would also be limited by the current shear strength τ_f of the soil element as determined in Section 3.7.

3.6.4 Behavior of Liquefied Soils

Liquefied soils are considered to have residual shear stiffness and residual shear strength. In VERSAT-D2D, the shear strength (S_{u_liq}) and the shear modulus (G_{liq}) of liquefied soil are defined using the following equations:

$$[3.34] \quad S_{u_liq} = c_{liq} + k_{liq} \sigma_{v0}'$$

$$[3.35] \quad G_{liq} = K_{g_liq} \bullet S_{u_liq}$$

Where:

c_{liq}, k_{liq} = shear strength constants of liquefied soils;

K_{g_liq} = shear modulus constant of liquefied soils; and

σ_{v0}' = pre-existing effective vertical stress.

The shear stress - strain relationship of liquefied soils is also modelled using a hyperbolic model (Figure 7) as described in Section 3.4.2. G_{liq} and S_{u_liq} are used as the initial modulus and the ultimate shear stress, respectively, in the hyperbolic model.

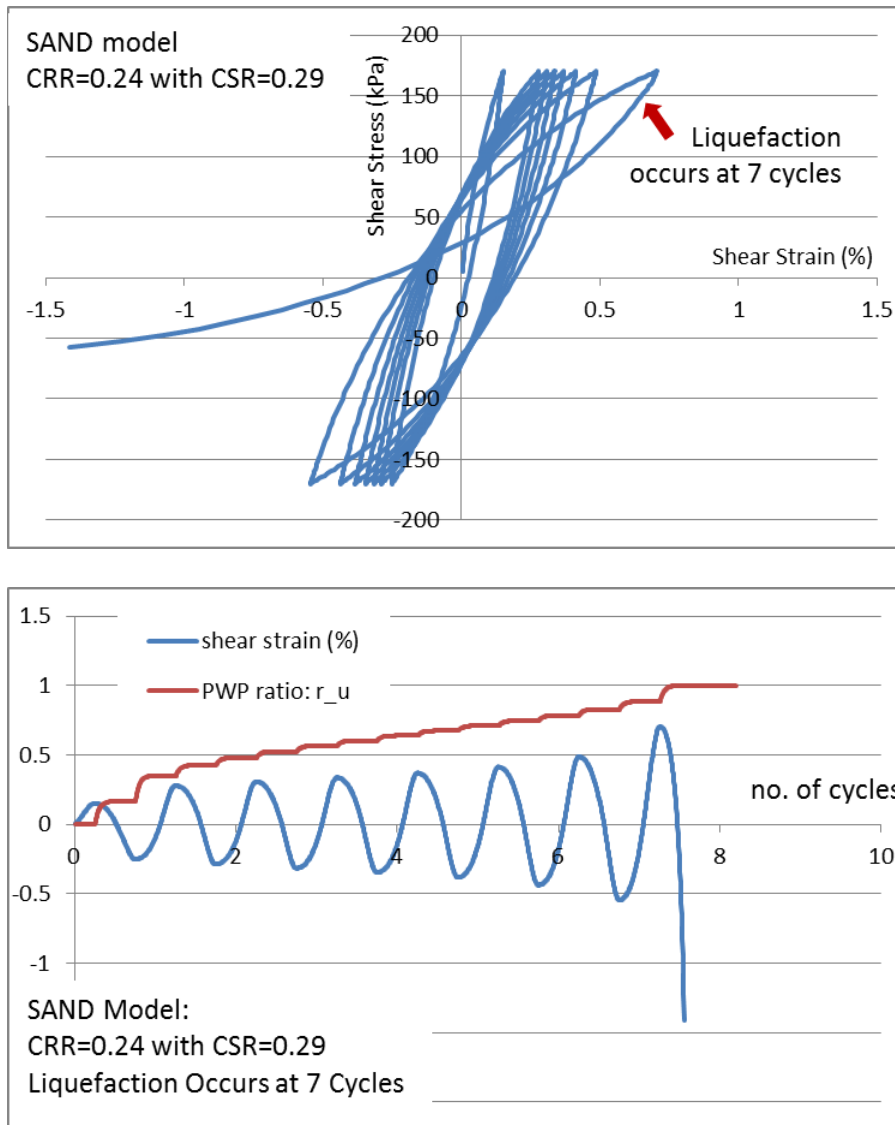


Figure 7 Shear Stress – Strain Curves for Liquefaction SAND Model

3.7 Determination of Shear Strength and Maximum Shear Stress

At each Gauss point in an element, current effective stresses are checked at each time step to ensure a stress state not violating the failure criterion, i.e., the maximum shear stress does not exceed the shear strength. The Mohr-Coulomb SAND Model and the Constant Strength CLAY Model, normally used to define shear strengths for sands and clays, respectively, are presented below.

3.7.1 Mohr-Coulomb SAND Model:

$$[3.36] \quad \tau_f = c \cdot \cos \phi + \frac{(\sigma_x + \sigma_y)}{2} \sin \phi$$

Where



σ_x, σ_y = current normal stresses in horizontal (X) and vertical (Y) directions, respectively;

c, ϕ = cohesion and friction angle of the soils, respectively;

The Mohr - Coulomb SAND Model is used to simulate material shear strengths that are functions of strength parameters as well as stresses induced by loading.

In an effective stress dynamic analysis, the current effective stresses (σ') are used in equation [3.36]. The shear strength of SAND Model would decrease as dynamic pore water pressure (u) builds up with time during dynamic loading.

3.7.2 Constant Strength CLAY Model:

In either a total stress or an effective stress dynamic analysis, the shear strength of Clay Model remains unchanged (constant) during dynamic loading, and it is a function of the strength parameters and the pre-existing stresses.

The shear strength of the Clay Model is calculated by:

$$[3.37a] \quad \tau_f = c \bullet \cos \phi + \frac{(\sigma_x' + \sigma_y')}{2} \sin \phi$$

$$[3.37b] \quad \tau_f = c + k\sigma_{v0}'$$

Where

c, ϕ = cohesion and friction angle of the soils, respectively;

c, k = shear strength constants that would be derived from results of field vane shear tests or laboratory direct simple shear tests where horizontal stresses are not well defined;

σ_x', σ_y' = pre-existing effective horizontal (X) and vertical (Y) stresses, respectively; and

σ_{v0}' = pre-existing effective vertical stress ($\sigma_{v0}' = \sigma_y'$).

Equation [3.37a] is applicable to Clay Model using strength parameters of c and ϕ ; and equation [3.37b] is applied when strength parameters c and k are input.

3.7.3 Maximum Static Plus Dynamic Shear Stress

The maximum static plus dynamic shear stress, τ_{\max} , is calculated using

$$[3.38a] \quad \tau_{\max} = \sqrt{\frac{1}{4}(\sigma_y - \sigma_x)^2 + \tau_{xy}^2}$$

Where

σ_x, σ_y = current normal stresses in horizontal (X) and vertical (Y) directions, respectively;

τ_{xy} = current shear stress in the XoY plane.

3.7.4 Maximum Shear Strain

In each time step of a dynamic analysis, the maximum shear strain, γ_{max} , is calculated using:

$$\gamma_{max} = \sqrt{(\varepsilon_y - \varepsilon_x)^2 + \gamma_{xy}^2}$$

[3.38b]

Where

$\varepsilon_x, \varepsilon_y$ = current normal strain in horizontal (X) and vertical (Y) directions, respectively.

γ_{xy} = current shear strain in the XoY plane.

3.8 Bending Elements for Structural Members

Beam elements are used to model the bending behavior of structural members such as sheet piles or tunnel walls. The bending stiffness of a beam element is given by

$$[3.39] \quad [K] = \frac{EI}{L^3} \begin{bmatrix} 12 & 6L & -12 & 6L \\ 6L & 4L^2 & -6L & 2L^2 \\ -12 & -6L & 12 & -6L \\ 6L & 2L^2 & -6L & 4L^2 \end{bmatrix}$$

Where

E = Young's modulus of the structural member (the beam), and $E = K_E * P_a$;

I = the bending moment of inertia of the beam per unit width⁷;

L = length of the beam element.

The axial stiffness of the beam element is given by

$$[3.40] \quad K_A = R_b \frac{EA}{L}$$

Where:

A = sectional area of the beam

R_b = a reduction factor used to reduce the axial stiffness of the beam. The use of a R_b value from 0 to 1 can simulate a variable degree of frictions between the structural members and the surrounding soils.

⁷ For example, $I=1/12*bh^3$ is for a rectangular section with a width of b and a height of h; and $I=1/64\pi* d^4$ (where $\pi=3.1416$) is correct for a circular section having a diameter of d. However, they would require some adjustments in a 2D plane-strain application ($I_{2D}=I_{pile}/s$ and $M_{pile} = M_{2D} * s$, where s represents the spacing of piles in the 3rd direction and M represents bending moment).

The beam elements can be used to simulate approximately the bending behavior of one row or multiple rows of piles distributed in the direction perpendicular to the 2D XOY plane. However, appropriate adjustments in structural properties would be needed since the piles do not form a continuous pile-wall in the direction perpendicular to the 2D XOY plane. Only a sheet pile wall does.

Beam elements can be orientated in any direction within the 2D XOY plane.

The bending moment, M , and shear force, Q , at the center of a beam element are computed by the program. The shear force within a finite beam element is constant. The bending moment at the first node (M_i) and at the second node (M_j) can be calculated using the following equations:

$$[3.41a] \quad M_i = M - 0.5 Q L$$

$$[3.41b] \quad M_j = M + 0.5 Q L$$

3.9 Spring Elements for Structural Truss or Bar

Elastic truss elements, or spring/bar elements, can be used to model anchors, struts or shoring supports. The axial stiffness of a truss element is defined by

$$[3.42] \quad K_A = \frac{EA}{L}$$

Where

E = Young's modulus of the structural members (the truss), and $E = K_E * P_a$;

A = sectional area of the truss;

L = the length of the truss element.

Appropriate adjustments in structural properties would be needed when truss elements are used to model structural members, such as struts, that are not continuous in the direction perpendicular to the 2D XOY plane.

The truss elements can be orientated in any direction within the 2D XOY plane.

3.10 Updated Lagrangian Analysis

The geometry of a mesh is continuously updated during the calculation when the updated Lagrangian analysis is used. This option is provided for solving problems involving large strain deformations.

3.11 Gravity On and Off

Normally gravity force is always acting downward in the model. Dynamic force equilibrium is maintained including gravity force and internal force consisting of soil effective stresses and

pore water pressures. Gravity force can be set off for analyses of structures not involving gravity.

3.12 Boundary Conditions

In a dynamic analysis, three boundary conditions are available:

- Fixed boundary,
- Free-field stress boundary,
- Constrained displacement boundary, and
- Viscous boundary (see Section 4 for more details).

3.12.1 Fixed Boundary

A fixed boundary consists of any nodes that are fixed (zero) in displacements for both X and Y directions. For the case of base excitation, input motions are applied at the fixed boundary, and displacements relative to the fixed boundary are computed. For a non-base-excitation case, absolute displacements at the fixed boundary are set to zero at all time.

A fixed boundary, either at the base or along sides of a model, may cause wave/energy reflection at the boundary. Therefore, a fixed boundary should be applied far away from the area of interest so that soil material damping is sufficient to absorb any energy reflected back from the boundary.

3.12.2 Free-Field Stress Boundary

The free-field stress boundary, with a fixed Y-displacement and a free X-displacement, is designed to approximately model the response of side (lateral) boundaries when they are not placed sufficient far away from area of interest. The free-field stresses, including horizontal normal stress (σ_x) and the shear stress τ_{xy} , are applied on the boundary and updated during the dynamic analysis.

3.12.3 Constrained Displacement Boundary

Constrained displacement boundary consists of nodes with a fixed Y-displacement and a free X-displacement but without applying free-field stress on the boundary. This boundary condition may be used to reduce wave/energy reflection from the lateral boundary for dynamic analyses not involving gravity force. Use of this boundary condition with gravity on may result in collapse at the side boundary.

3.13 Dynamic Point Loads

For problems not involving earthquake loading, dynamic loads can be applied at any nodes using the degrees of freedom associated with a node number, i.e., nldof. The degrees of freedom associated with a node can be found in the output file for geometry data, i.e., a file with an extension of OUG.

3.14 Dynamic Analysis of 1D Soil Columns

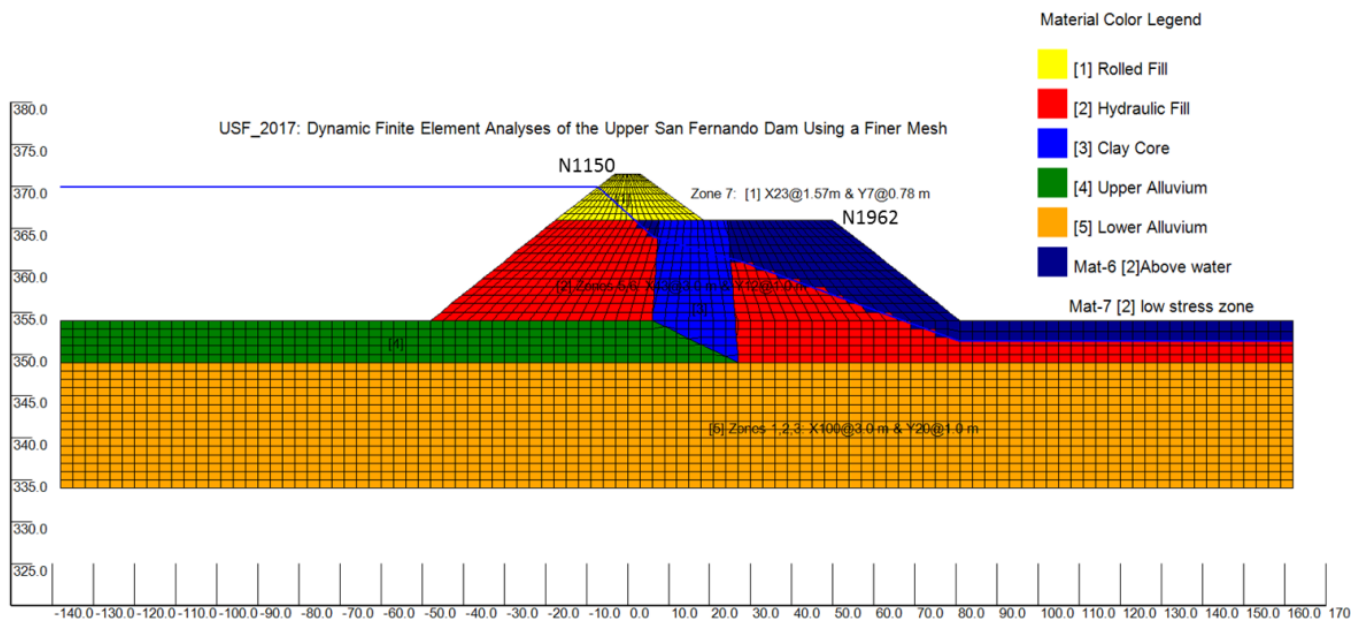
Refer to Section 4.6 in the VERSAT-2D Vol. 2 User Manual for details.

3.15 Units and Signs

This section is the same as Section 2.12.

3.16 Dynamic Analysis of Upper San Fernando Dam under 1971 Earthquake

The 2017 refined model is shown below; see Appendix B and also in “Ex_d2017_USF-Dam_2704-Elem” in VERSAT-2D_2019_Examples for detailed analysis input files and results.



4.0 Advanced Options for VERSAT-2D Dynamic Analysis

Advanced options for dynamic analysis, including the Outcropping Velocity Input Option and the SILT Model Option, are made available in VERSAT-2D since 2011.

4.1 Outcropping Velocity Input

4.1.1 Equation of Motions and its Formulations

For a finite element model having an elastic base instead of a rigid base, outcropping velocity time histories are applied directly at the base of the model through a viscous boundary (i.e., energy absorbing boundary or elastic base boundary). The viscous boundary developed by Lysmer and Kuhlemeyer (1969) is used in VERSAT-2D, and it consists of viscous dashpots attached to the model base. One dashpot is independently attached to one base node in the finite element model in the X direction (i.e., the shear direction). The viscous boundary is fixed to zero displacement in the Y direction (i.e., the normal direction).

The equation of motions (equation [3.1]) presented for models with acceleration input is also applicable for models with velocity input, and the equation is rewritten as follows:

$$[4.1] \quad [M]\{\Delta a\} + [C]\{\Delta v\} + [K]\{\Delta \delta\} = \{\Delta P\}$$

Where

[M] = mass matrices

[C] = viscous damping matrices

[K] = tangent stiffness matrices

[\Delta\delta] = incremental displacement matrices

[\Delta v] = incremental velocity matrices

[\Delta a] = incremental acceleration matrices

[\Delta P] = incremental external load matrices

However, constitution of the equation of motions is quite different for the two types of ground motion input. Firstly, displacement (also velocity and acceleration) at the model base with acceleration input is known and equal to the input motions. The ground motion (displacement, velocity and acceleration) at the viscous boundary with the velocity input are the within motions to be determined by the analysis. Secondly, the calculation of external load matrix [\Delta P] is also different for the two input motion methods. With acceleration input at the rigid base, incremental inertial forces on the soil mass caused by base accelerations are computed using the Newton's law and applied as [\Delta P]. With the velocity input at the elastic base, incremental shear forces at the base nodes are determined and applied as [\Delta P].

The method of Joyner and Chen (1975) for including the effect of finite rigidity of the base material on shear stress at the base is incorporated in VERSAT-2D. The method basically evaluates the shear stress, τ_B , being transmitting across the base boundary between the soil deposit and the underlying elastic medium. It is assumed that the propagating shear waves are plane waves traveling vertically.

The elastic base model with the viscous boundary is presented in Figure 8. The shear stress, τ_B , at the viscous boundary is determined by

$$[4.2] \quad \tau_B = \rho_b V_s (2v_I - v_b)$$

Where:

ρ_b = mass density of the elastic base material,

V_s = shear wave velocity of the elastic base material,

v_I = particle velocity at the boundary due to the incident shear wave, and

v_b = within particle velocity at the boundary.

The particle velocity at the boundary, v_b , together with displacement and acceleration at the boundary, is unknown and to be determined by the analysis. Thus, equation [4.2] is divided into two components:

$$[4.3a] \quad \tau_{BI} = \rho_b V_s v_o$$

$$[4.3b] \quad \tau_{Bb} = -\rho_b V_s v_b$$

Where

v_o = outcropping particle velocity of the elastic base material, and

τ_B = $\tau_{BI} + \tau_{Bb}$.

The shear force at i^{th} node on the boundary, derived from equation [4.3a], is then applied as external load in equation [4.1], i.e.

$$[4.4] \quad \Delta P_i = A_i \rho_b V_s \Delta v_o$$

Where

Δv_o = incremental outcropping particle velocity of the elastic base material, and

A_i = area of the base boundary represented by i^{th} node.

On the other hand, the shear force at i^{th} node derived from equation [4.3b] is moved to the left side of equation [4.1]. The viscous damping constant, C_i , corresponding to the unknown boundary velocity v_{bi} , is then determined to be

$$[4.5] \quad C_i = A_i \rho_b V_s$$

The viscous damping constant, C_i , computed from equation [4.5] is directly added to the damping matrix $[C]$ of equation [4.1] as an addition to the diagonal term corresponding to its boundary velocity v_{bi} .

The stiffness matrix $[K]$ in equation [4.1] is not affected by the viscous boundary; the diagonal terms of the mass matrix $[M]$ corresponding to the nodes on the viscous boundary are set to zero in the dynamic analysis.

The velocity input option may be used to examine the influence of the rigidity of the underlying elastic medium on ground motions transmitting to the soil deposit. The displacements, velocities and accelerations determined from this type of analysis are absolute, i.e., not relative to the base, for every node in the finite element model.

The velocity input option in VERSAT-2D requires that the base boundary be horizontal and free-field stress boundaries (if exist) be used for vertical side boundaries.

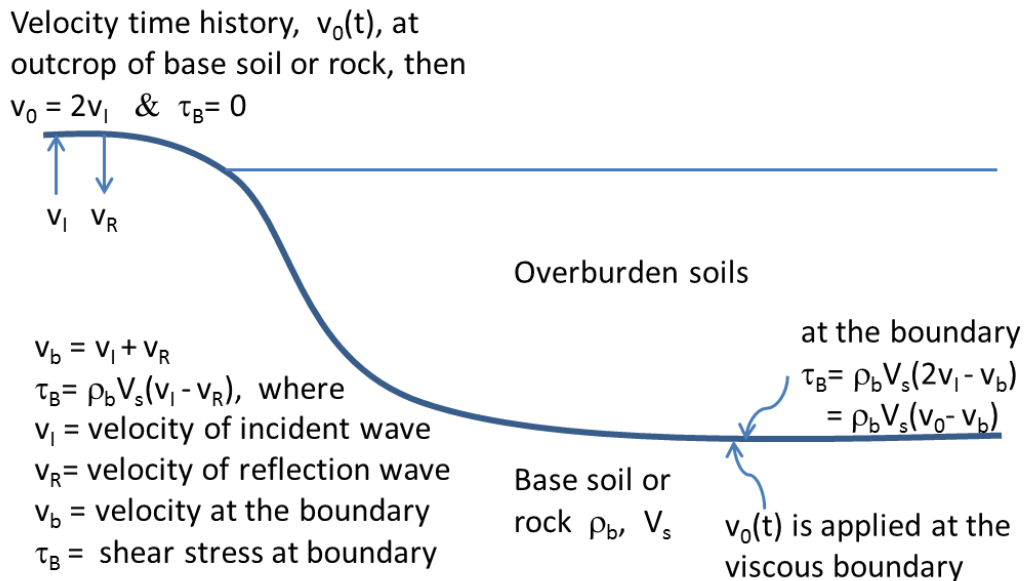


Figure 8 Elastic base model with a viscous boundary



4.1.2 Traveling of Input Motion at the Viscous Base

For acceleration input at the base, input motions (i.e., inertial forces) on the entire model must be applied at the same instance in time; however, for velocity input at the base, input velocity time history (i.e., shear forces) can be applied to a node on the viscous base starting at any specified instance in time.

In VERSAT-2D, a simple method is used to simulate traveling of input motion at the viscous base. The method assumes that the same velocity trace (time history) is applied to i^{th} node on the viscous boundary at a time instance, t_i , proportional to its distance to a user specified point, i.e.

$$[4.6] \quad t_i = \frac{|x_i - x_0|}{V_{\text{wave}}}$$

Where

x_0 = a user defined X coordinate where the velocity trace is applied at $t_i = 0$;

x_i = the X coordinate of i^{th} node on the viscous base;

V_{wave} = speed of wave traveling along the viscous base.

4.1.3 An Example Using Outcropping Velocity Input and Comparing with SHAKE

Computed response for a 1D soil column (147.5 m high) with a rigid base are compared in Figure 9 with that for the same 1D column on an elastic base with a V_s of 100,000 m/s. The analysis for the rigid base model is conducted by applying an acceleration time history of an input ground motion to the model; while a velocity time history of the input ground motion is used for the elastic base model. See “Ex_1D_Dyn_Elastic-vs-Rigid_base” in VERSAT-2D_2019_Examples for detailed input and output files.

As expected and shown on the top plot in Figure 9, computed absolute ground displacements at the base of the elastic model are practically identical to the displacement time history of the input ground motion (i.e., input displacement for the rigid base model) because of the very high shear velocity of the elastic base. Furthermore, as shown on the bottom plot in Figure 9, absolute displacements at the top of the 1D column using the elastic base model (directly computed by the program) are also practically identical to those computed using the rigid base model. Absolute displacement for a rigid base model is the summation of computed displacement (i.e., relative to the rigid base) and the input ground displacement at the base.

The effects of an elastic base with $V_s=450$ m/s on ground response are illustrated in Figure 10, and the results are compared with analysis results from SHAKE (Schnabel et al. 1972). At a low-moderate level of earthquake shaking, SHAKE equivalent linear approximation is able to produce very good representation of true soil nonlinear hysteresis behavior. More details of this comparison are provided in Appendix A of this document (Ex_1D_Elastic-base_Compare-to-SHAKE).



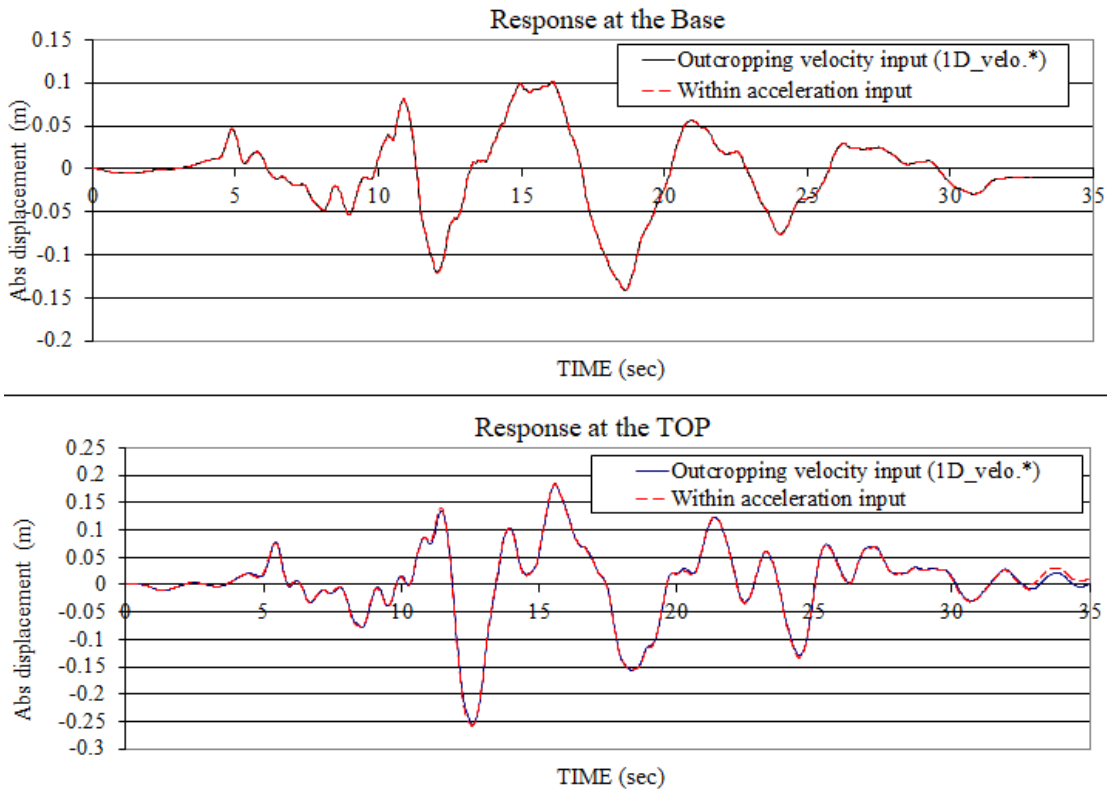


Figure 9 Response of a 1D Soil Column: Acceleration versus outcropping velocity input

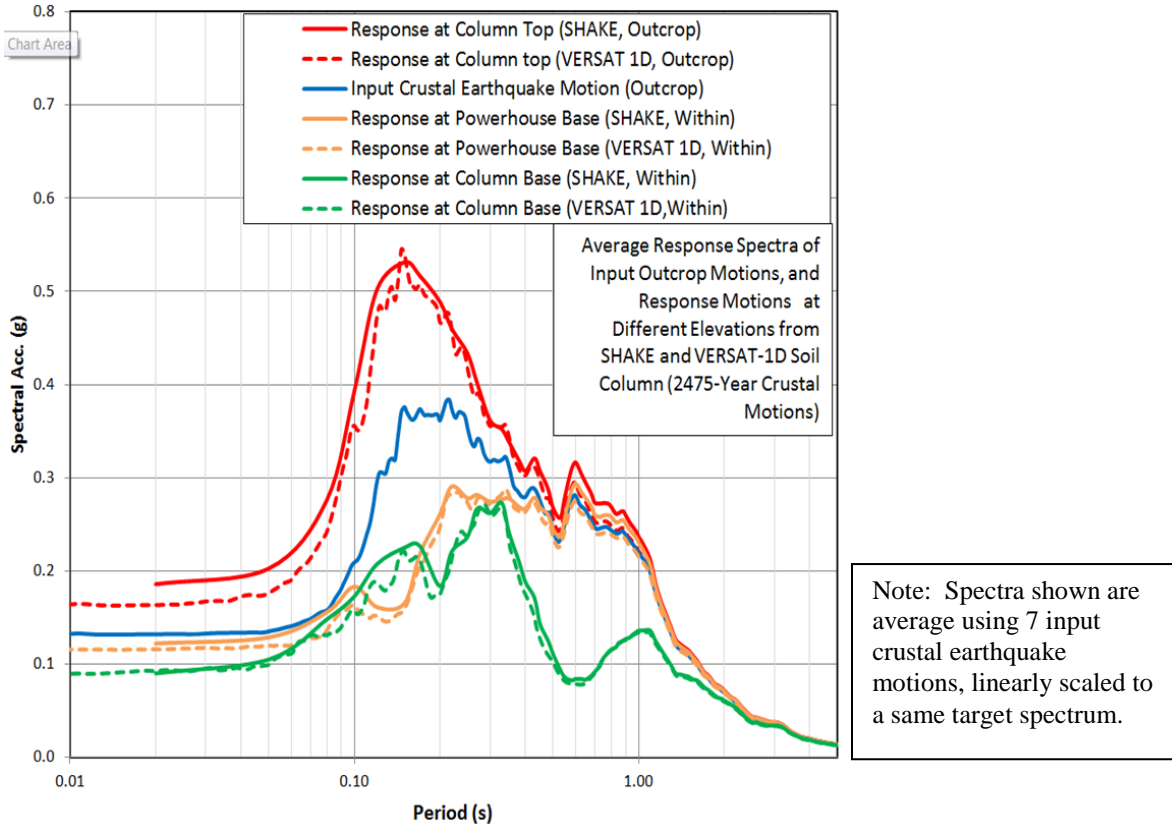


Figure 10 Results of SHAKE & VERSAT-1D Soil Column with an elastic base, $V_s=450$ m/s



4.2 SILT Model - updated in v.2016.6.18

4.2.1 Shear Stress - Strain Relationship for SILT Model

VERSAT-2D simulates the shear stress-strain relationship for silts by simulating strain-softening response with increasing cycles of stress but hardening response within a particular stress cycle. When the pore water pressure ratio (r_u) is less than the threshold value, $r_{u,0}$, the hyperbolic stress-strain model as described in Section 3.4 is used. When r_u exceeds the threshold value of $r_{u,0}$, a strain-softening model is then used in the analysis (Finn and Wu, 2013; Wu 2015).

The relationship between shear stress, τ_{xy} , and shear strain, γ , for the hardening condition within a stress cycle, at r_u , is assumed to be nonlinear and hyperbolic (see Figure 11) as follows:

$$[4.7] \quad \tau_{xy} = \frac{G_h \gamma}{1 - |\gamma|/\gamma_h}$$

$$[4.8] \quad G_h = \sqrt{1 - r_u} G_{max} \cdot (0.1 - 0.075 r_u)$$

$$[4.9] \quad \gamma_h = \text{Max}(0.05, \gamma_{H0} - \frac{\tau_{f0}}{s_{u,liq}}) + \gamma_{H0} \cdot r_u$$

Where,

G_h = initial shear modulus of the hardening hyperbolic curve

γ_h = ultimate shear strain (%) of the hardening hyperbolic curve

r_u = pore water pressure ratio, calculated using Eq. [3.31] as for SAND Model

τ_{f0} = the static shear strength (τ_f) prior to shaking, i.e., at $t = 0$

$S_{u,liq}$ = post-liquefaction or residual shear strength, see Section 4.2.4

γ_{H0} = input, shear strain (%) to trigger initial strain softening, typically 3.5 – 5%

In the SILT Model, $r_{u,0}$ and γ_{H0} are the two input parameters that should be assigned by the user. All other parameters are self-calculated by the program or defined elsewhere.

γ_{H0}	$\frac{\tau_f \text{ at } t=0}{s_{u,liq}}$	γ_h (%) @ $r_u = 0$	γ_h (%) @ $r_u = 0.95$
3.5%	1	2.5	6
	1.5	2	5.3
	3.5	0.05	3.4
5.0%	1	4	8.75
	3	2	6.75
	5 **	0.05	4.8

** Increasing from 1 to 5 shows ductile to brittle

The above empirical relationships were developed by fitting to data from laboratory cyclic tests on silts. For either non-level ground conditions where static shear stress exists or for a level ground condition where $\tau_{st} = 0$, the ultimate strain (γ_h) is always referenced from zero shear strains.

4.2.2 Shear Strengths for SILT Model

Shear strengths for the SILT Model are determined either using the Mohr–Coulomb SAND Model or Constant Strength Clay Model. The following rules are applied:

- Use of parameters c and ϕ : Mohr-Coulomb SAND Model with equation (3.36); or
- Use of parameters c and k : Constant Strength CLAY Model with equation (3.37b).

A comparison of features for the SAND Model and the SILT Model is presented in Table 1.

4.2.3 Dynamic Pore Water Pressures and Liquefaction for SILT Model

SILT Model can always develop dynamic pore water pressure, u , regardless of shear strength models adopted for the silts (see Table 1).

The three dynamic pore water pressure models, developed for SAND Model and described in Section 3.5, are equally applicable for the SILT Model.

For the SILT model, initial strain softening (or liquefaction) is triggered using one of the three criteria:

- Cumulative dynamic pore water pressure ratio exceeds 0.95, i.e., $r_u \geq 0.95$, or
- Peak shear strain (γ_{xy}) exceeds the threshold strain, γ_{H0} , or
- Peak shear stress (τ_{xy}) exceeds the dynamic shear strength (where τ_{15}^{crit} is defined in Eq. [3.27] and α is the shear stress conversion constant in Section 3.5.5):

$$[4.10] \quad \tau_{xy} > \sigma_{v0}' \cdot [\tau_{15}^{crit} \cdot (15)^{1/\alpha}]$$

4.2.4 Post Liquefaction Simulation for SILT model

Once initial strain softening is triggered, the shear strength of the silt is reduced gradually to S_{u_liq} as the shear strain increases towards γ_H . The fraction of strength reduction is determined by the fraction of strain increment and a strength reduction factor (also called a fit factor, or S_{r_fac}), an input parameter by the user.

Fraction of strength reduction is calculated using an exponential function and



$$= (\text{fraction of strain increment})^{sr_fac}$$

The fraction (0 – 1) of strength reduction is linear with the fraction (0 – 1) of strain increment when $S_{r_fac} = 1$, and it becomes nonlinear when $S_{r_fac} > 1$ (slow reduction) or when $0 < S_{r_fac} < 1$ (fast reduction).

The minimum strength of the liquefied silt, i.e., the residual strength is reached and then kept constant (Figure 11) when the shear strain reaches or exceeds γ_H :

$$[4.11] \quad S_{u_liq} = c_{liq} + k_{liq} \cdot \sigma_{v0}'$$

S_{u_liq} = the residual strength of the silt, also referred as S_{ur} ;

γ_H = shear strain γ_{xy} (%), an input parameter, corresponding to the residual strength.

Equation [4.7] is also used for stress – strain relationship of the silt after liquefaction. The ultimate strain (γ_h) is set to be 2 – 3.5%, and the initial shear modulus (G_h) of the hardening hyperbolic curve is set to be 2.5% of the shear modulus of the liquefied silt (G_{liq} in Eq. [3.35]):

$$[4.12] \quad G_h = 0.025 * G_{liq}$$

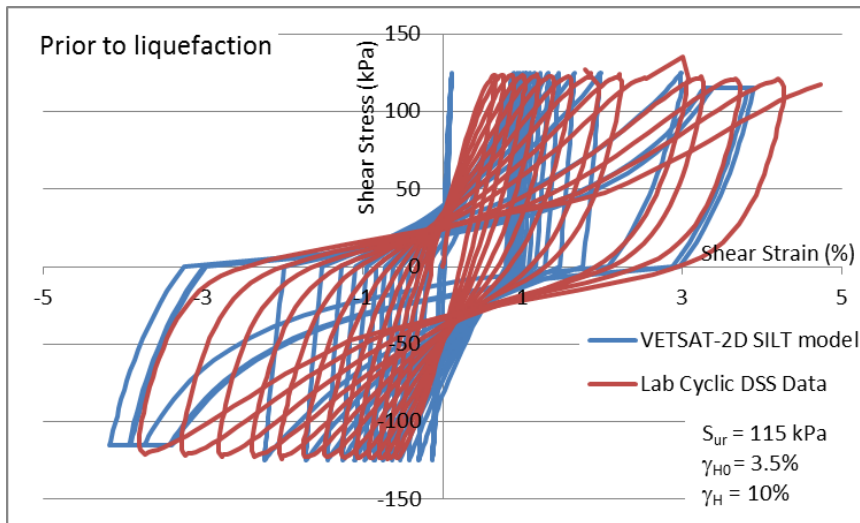
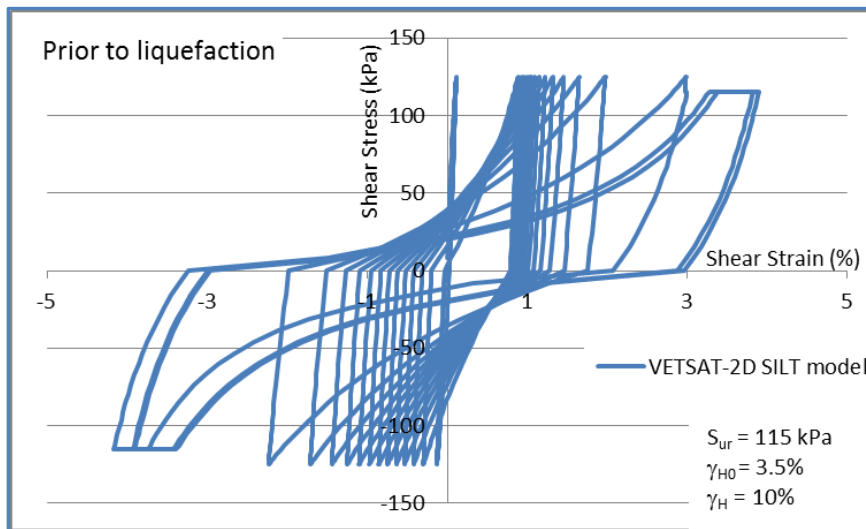
$$G_h = 2.5\% \cdot (K_{g_liq} \cdot S_{u_liq}) \quad (K_{g_liq} = 100 \text{ to } 400 \text{ as for SAND Model})$$

Table 1 Comparison of Features for SAND Model and SILT Model

Features	SAND Model (c, ϕ)	SILT Model	
		parameters (c, ϕ)	parameters (c, k)
Shear stress – strain Relationship	hyperbolic	Hyperbolic & strain-softening	hyperbolic & strain-softening
Dynamic pore water pressure, u	Yes	Yes	Yes
u in force equilibrium	Yes	Yes	Yes
Reduction of stiffness	Yes	Yes	Yes ⁽¹⁾
Shear strength prior to liquefaction, τ_f ⁽²⁾	$\tau_f = f(\sigma', c, \phi)$	$\tau_f = f(\sigma', c, \phi)$	$\tau_f = c + k \cdot \sigma_{v0}'$
	Reduced with u	Reduced with u	No change with u
Trigger of liquefaction	Yes	Yes	Yes
Trigger by strain	No	Yes When $\gamma_{xy} > \gamma_{H0}$	Yes When $\gamma_{xy} > \gamma_{H0}$
Post-liquefaction shear strength, S_{u_liq} (or S_{ur})	$S_{u_liq} = c_{liq} + k_{liq} \cdot \sigma_{v0}'$ - Invoked at trigger	$S_{u_liq} = c_{liq} + k_{liq} \cdot \sigma_{v0}'$ - Reduced from τ_f with γ_{xy} invoked at $\gamma_{xy} \geq \gamma_H$	$S_{u_liq} = c_{liq} + k_{liq} \cdot \sigma_{v0}'$ - Reduced from τ_f with γ_{xy} invoked at $\gamma_{xy} \geq \gamma_H$



- (1) In hyperbolic portion (i.e., for $r_u < r_{u,0}$), equations [3.32] and [3.33] are used (i.e., shear modulus is reduced as u increases. When SILT model is invoked (i.e., for $r_u > r_{u,0}$), shear stiffness is governed by equations [4.8] and [4.9], and is also reduced as u increases.
- (2) $\sigma' = f(u)$, current effective stresses; $\sigma'_0 =$ pre-existing effective stresses



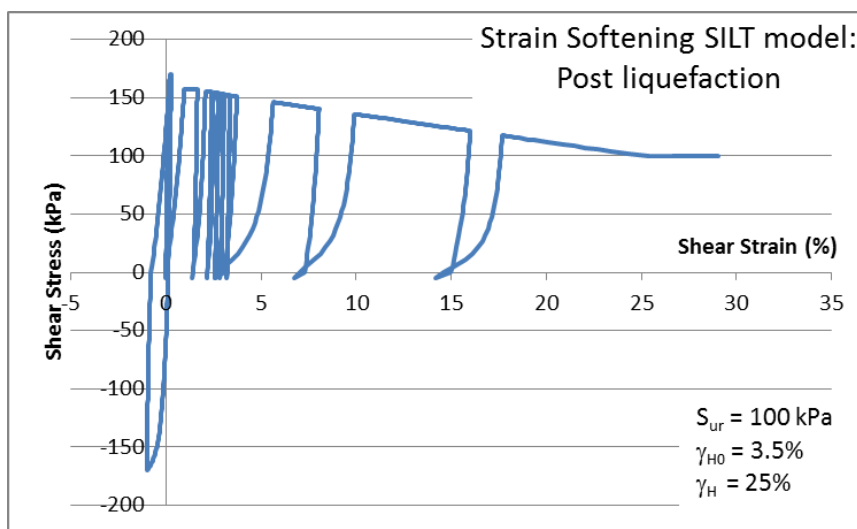


Figure 11 Shear Stress – Strain Curves for Strain-Softening SILT Model

4.3 Probabilistic Seismic Performance Analysis (PSPA)

4.3.1 PSPA Method (version 2019.05 and later)

In many cases, it is desirable to generate performance hazard curves (such as displacement hazard) for a structure located in an area with seismic hazard contributions from both the subduction Interface (e.g., Magnitude 9 or M9) and the Non-Interface (e.g., M7) crustal or subduction intra-slab earthquakes.

To efficiently carry out the probabilistic approach, dynamic time-history analyses would be carried out in an automation setup where a set of ground motion records (such as 11 Interface records plus 11 Non-Interface records) can be applied automatically to one model at various levels of probability levels. For instance, the same suite of ground motion records can be scaled linearly at different scale factors to simulate seismic hazards at 1/475-yr, 1/1000-yr, 1/2475-yr, 1/5000-yr, 1/10,000-yr and 1/50,000-yr. The procedure of automation was demonstrated in a technical article “Probabilistic approach to design of seismic upgrade to withstand both crustal and subduction earthquake sources” (Wu 2018), where a total of 264 dynamic analyses were conducted in about 3 days (24 hours a day) of computer time on a PC.

Results of dynamic analyses (Wu 2018) for the Upper San Fernando (USF) dam, assumed to be relocated in Campbell River area of BC, indicated that displacement hazard contributions for all earthquake sources are dominated by the M9 Interface Event; and the earthquake magnitude (i.e., duration) has a much greater impact on seismic displacement than UHS.

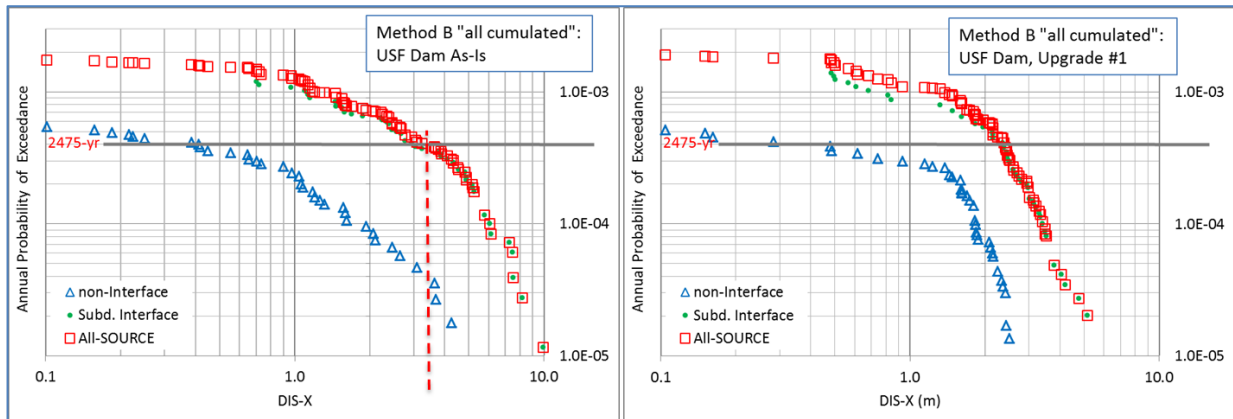
The analysis results in Figure 12 (after Wu 2018) also indicated that, at the dam crest the displacement hazard fractions at the 1/2475-yr level (AEF of 0.000404 or 4.04×10^{-4}) consisted of the following:

- 0.000371 or 3.71×10^{-4} from the Interface earthquake source, i.e., 1/2695-yr

- 0.000033 or 0.33×10^{-4} from Non-Interface earthquake source, i.e., 1/30,300-yr

The above observation is significant. It implies that for design of 1/2475-yr hazard level, the design ground motions would be developed to target at 1/2695-yr Interface spectra, or at 1/30,300-yr Non-Interface spectra. It is noted that the 1/2695-yr Interface spectral acceleration (S_a) is significantly (about 25%) lower than the 1/2475-yr UHS at $T=0.015$ sec, and it is still lower (for about 10%) at $T=1.0$ sec.

Figure 12 Displacement Hazard Curves from the probabilistic analyses (after Wu 2018)



4.3.2 Input and Output Files

See Section 4.10 in “VERSAT-2D Volume 2: USER MANUAL” for more instructions on how to perform the PSPA with one more input file.

4.4 Use ICHANG=3 to Input Soil Strength by Element

This function is available for version 2019.05 and later.

In some cases, it is not sufficient to define strength of soils by using the soil material zone; the user may wish to input soil strength of an individual element based on its location or its in-situ shear and/or vertical stresses. This can be achieved by using the “ICHANG=3” option.

This “ICHANG=3” option is only valid in a dynamic analysis, i.e., not applicable to a static analysis. Its functionality is the same as “Non-linear Effective Stress Analysis” or ICHANG=2.

See Section 4.11 in the User Manual to learn how to invoke the option in VERSAT-2D Processor.

5.0 List of References <http://www.wutecgeo.com/pubv2d.aspx> for VERSAT-2D application

1. BC Hydro 2008. Dynamic time-history analyses of seismic induced soil liquefaction and ground deformations for Cheakumas Dam. Engineering Report
2. BC Hydro 2010. VERSAT-2D dynamic response analyses, including horizontal and vertical ground motions, for a new control building on Seton Dam, Engineering Report
3. BC Hydro, 2012. VERSAT-2D dynamic time-history analysis for seismic upgrade design of the Ruskin Dam Right Abutment, Engineering Report(s)
4. BC Hydro, 2013. VERSAT-2D dynamic time-history analyses of John Hart Middle Earthfill Dam on Over-consolidated Silts with Cyclic Strain Softening or Liquefaction. Engineering Report
5. BC Hydro 2016. VERSAT-2D Seismic Stability and Deformation Analyses of WAC Bennett Dam, BC Hydro WAC Bennett Dam Expert Engineering Panel Report, March 24, 2016
6. Bhatia, S. K. (1980), "The verification of relationships for effective stress method to evaluate liquefaction potential of saturated sands," Ph.D thesis, Department of Civil Engineering, the University of British Columbia, Vancouver, B.C., Canada
7. Byrne, P. M. (1991), "A cyclic shear-volume coupling and pore pressure model for sand," Proceedings, 2nd international conference on Recent Advances in Geotechnical Earthquake and Soil Dynamics, St. Louis, Missouri, March, Vol. 1, pp. 47-56.
8. Finn, W. D. Liam, Lee, W.L. and Martin, G.R. (1977) "An effective stress model for liquefaction", Journal of the Geotechnical Engineering Division, ASCE, Vol. 103, No. GT6
9. Finn, W.D.Liam, R.H., Ledbetter and Guoxi Wu, 1994. "Liquefaction in Silty Soils: Design and Analysis," Ground Failures under Seismic Conditions, ASCE Geotechnical Special Publication No 44, Atlanta, U.S.A., Oct., 1994, pp. 51-76
10. Finn W.D.Liam and Wu, Guoxi, 2013. Dynamic Analyses of an Earthfill Dam on Over-Consolidated Silt with Cyclic Strain Softening. Keynote Lecture, Seventh International Conference on Case Histories in Geotechnical Engineering, Chicago, US, April 29 - May 4.
11. Ishihara K. and Yoshimine M. (1992) "Evaluation of settlements in sand deposits following liquefaction during earthquakes", Soils and Foundations, Vol. 32, No. 1, pp. 173 – 188
12. Joyner, W.B. and Chen, A.F.T., 1975. "Calculation of Non-linear Ground Response in Earthquakes", Bull. Seism. Society America, Vol. 65, no. 5, 1315-1336, October.
13. Lysmer, J., and Kuhlemeyer R.L., 1969. "Finite Dynamic Model for Infinite Media," J. Eng. Mech. Div., ASCE, Vol. 95, 859-877, August.
14. Martin, G.R., Finn, W. D. Liam and Seed, H.B. (1975) "Fundamentals of liquefaction under cyclic loading", Journal of the Geotechnical Engineering Division, ASCE, Vol. 101, GT5
15. Sweeney, N. and Yan L. 2014. Dam Safety Upgrade of the Ruskin Dam Right Abutment, Canadian Dam Association 2014 Annual Conference, Alberta, Canada.



16. Seed, R.B. and Harder, L.F. (1990). SPT-Based Analysis of Cyclic Pore Pressure Generation and Undrained Residual Strength. H. Bolton Seed Memorial Symposium Proceedings, BiTech Publishers.
17. Seed, H.B., Martin, P.P., and Lysmer, J., (1976) "Pore-Water Pressure Changes During Soil Liquefaction," Journal of the Geotechnical Engineering Division, ASCE, Vol. 102, No. GT4, pp. 323 – 346.
18. Wu, Guoxi (1996) "Volume Change and Residual Pore Water Pressure of Saturated Granular Soils to Blast Loads", A research report submitted to Natural Sciences and Engineering Research Council of Canada.
19. Wu, G., 2001. Earthquake induced deformation analyses of the Upper San Fernando dam under the 1971 San Fernando earthquake. Canadian Geotechnical Journal, 38: 1 – 15
20. Wu, G., Fitzell, T., and Lister, D. 2006. Impacts of deep soft soils and lightweight fill approach embankments on the seismic design of the Hwy. 15 North Serpentine River Bridges, Surrey, B.C. Proceedings of the 59th Canadian Geotechnical Conference, Vancouver, pp. 596-601^[from VERSAT-2D]
21. Wu, G. 2010. Seismic soil pressures ^[from VERSAT-2D] on rigid walls with sloped backfills. Proceedings of the 5th International Conference on Recent Advances in Geotechnical Earthquake Engineering and Soil Dynamics, San Diego, California, US, May 24-29
22. Wu, G. 2015. Seismic Design of Dams, Encyclopedia of Earthquake Engineering published by Springer-Verlag B`erlin Heidelberg 2015
23. Wu, G. 2017. Probability approach for ground and structure response to GSC 2015 seismic hazard including crustal and subduction earthquake sources, A technical presentation on November 14, 2017 to Vancouver Geotechnical Society (VGS). The presentation is available at: <http://v-g-s.ca/20172018-lecture-series>
24. Wu, G. 2018. Probabilistic approach to design of seismic upgrade to withstand both crustal and subduction earthquake sources, Proceedings of the 25th Vancouver Geotechnical Society (VGS) Symposium on Ground Improvement, June. The presentation is available at: <http://v-g-s.ca/2018-proceedings>
25. Youd, T.L. et al. (21 authors), 2001. Liquefaction Resistance of Soils: Summary Report from the 1996 NCEER and 1998 NCEER/NSF Workshops on Evaluation of Liquefaction Resistance of Soils. Journal of Geotechnical and Geo-environmental Engineering, ASCE, Vol. 127, No. 10, pp.817-833

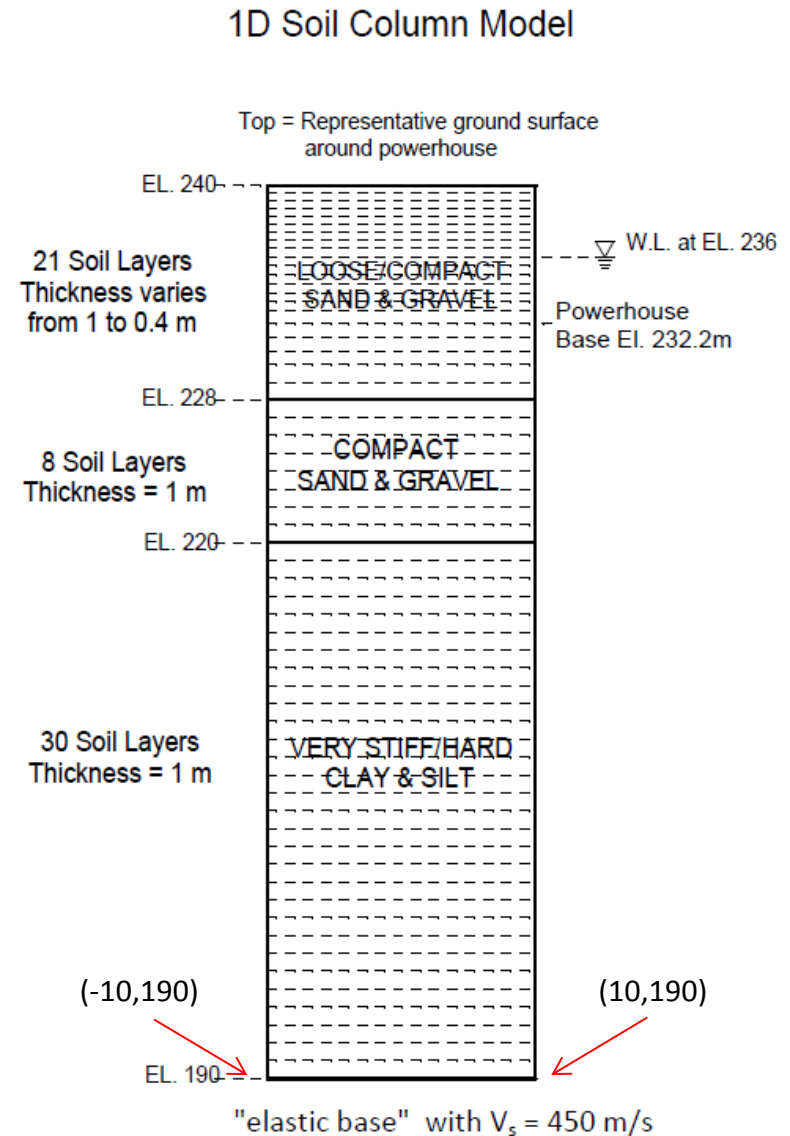


Appendix A: Comparing 1D Soil Column Analyses: SHAKE and VERSAT-1D



- 2.4 Example 2 – prepared in March 2018
Comparison between SHAKE and
VERSAT-1D at low-moderate level of
earthquake shaking:

1D soil column - MODEL



- 2.4 Example 2: Comparison between SHAKE and VERSAT-1D at low-moderate level of earthquake shaking: 7 input crustal ground motions

Table 2.1 Meta Data of the Seven Crustal Earthquake Records

No.	Short Name	NGA Record Number	Earthquake Name	Year	Station Name	Magnitude	Mechanism	Rjb (km)	Rrup (km)	Vs30 (m/sec)
1	FTR	63	"San Fernando"	1971	"Fairmont Dam"	6.6	Reverse	26	30	634
2	CPE	164	"Imperial Valley-06"	1979	"Cerro Prieto"	6.5	strike slip	15	15	472
3	SCN	369	"Coalinga-01"	1983	"Slack Canyon"	6.4	Reverse	26	27	648
4	SJR	472	"Morgan Hill"	1984	"San Justo Dam (R Abut)"	6.2	strike slip	32	32	544
5	G06	769	"Loma Prieta"	1989	"Gilroy Array #6"	6.9	Reverse Oblique	18	18	663
6	CHL	989	"Northridge-01"	1994	"LA - Chalon Rd"	6.7	Reverse	10	20	740
7	LV3	1029	"Northridge-01"	1994	"Leona Valley #3"	6.7	Reverse	37	37	499

Set	Dir	N	dt	Max.Accel.	Max. Vel.	Max. Disp.	Arias Int.	Duration
		points	[sec]	[g]	[m/s]	[m]	[m/s]	5%-95%[sec]
7 Crustal EQ Records - Horizontal (X) and Vertical (Z)								
1	X	6112	0.01	0.202	0.167	0.038	0.342	17.86
2	X	6382	0.01	0.131	0.082	0.041	0.562	33.7
3	X	5999	0.01	0.139	0.147	0.026	0.175	13.51
4	X	5673	0.005	0.125	0.131	0.071	0.408	21.98
5	X	7998	0.005	0.136	0.126	0.05	0.261	13.23
6	X	3107	0.01	0.106	0.087	0.017	0.183	9.08
7	X	1600	0.02	0.145	0.163	0.04	0.316	12.54

- 2.4 Example 2: Comparison between SHAKE and VERSAT-1D at low-moderate level of earthquake shaking: soil profiles and parameters

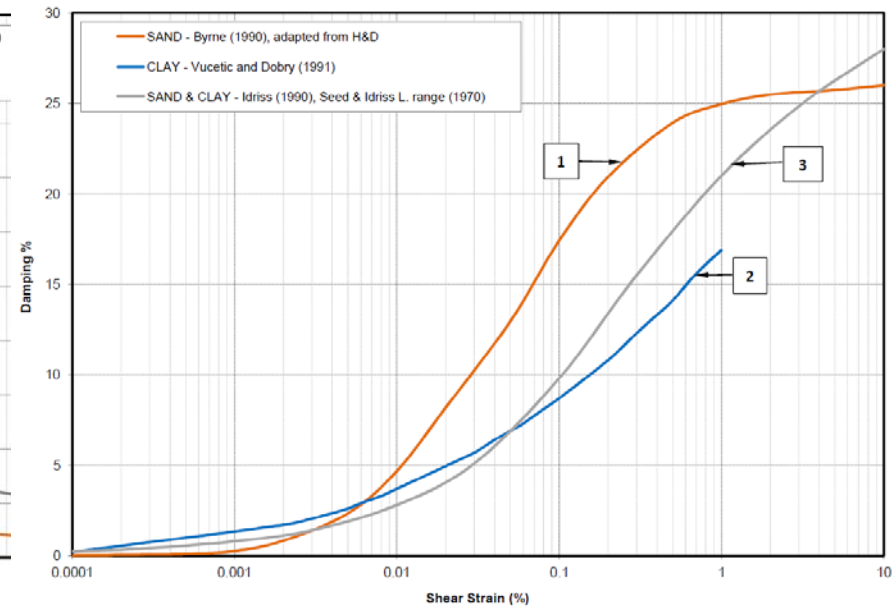
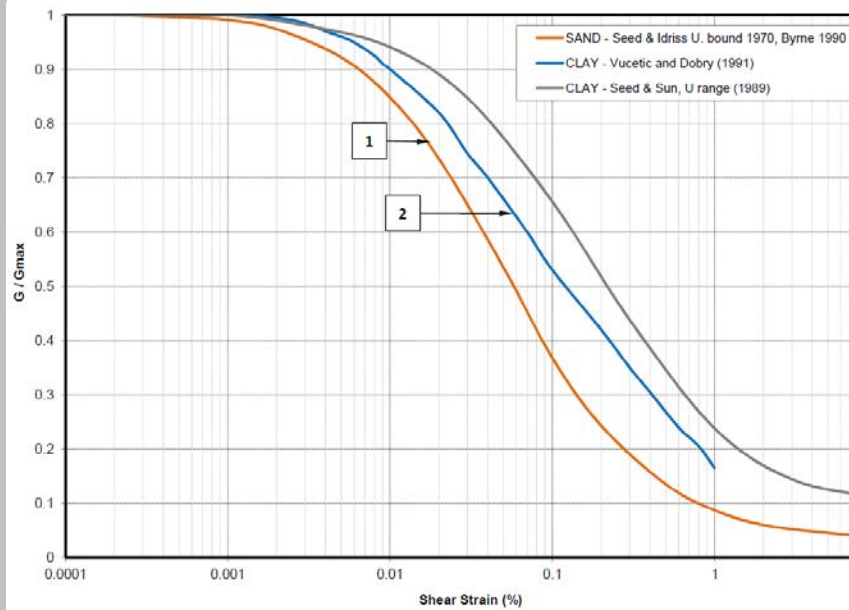
Table 2.2 Soil Unit Weights and Shear Wave Velocities for SHAKE and VERSAT-1D

No.	Soil Layer Description	Unit Weight (kN/m ³)	Shear Wave Velocity, V_s (m/s)
1a	Wet Loose to Compact Sand and Gravel (above water level)	19.5 (a.wt)	160
1b	Saturated Loose to Compact Sand and Gravel (below water level)	21.2 (b. wt)	300
3	Compact Gravel to Gravel	21.2	400
4	Very Stiff to Hard Clay and Silt	20.4	360
5	Very Dense/Hard Silt and Sand	21.7 ("elastic base" input)	450

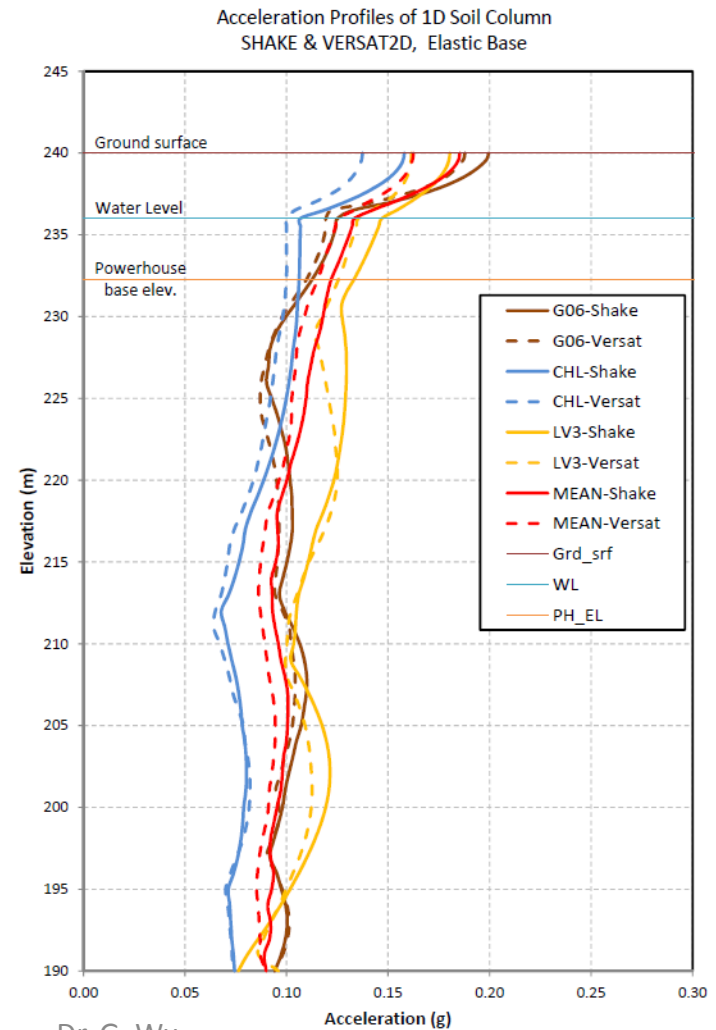
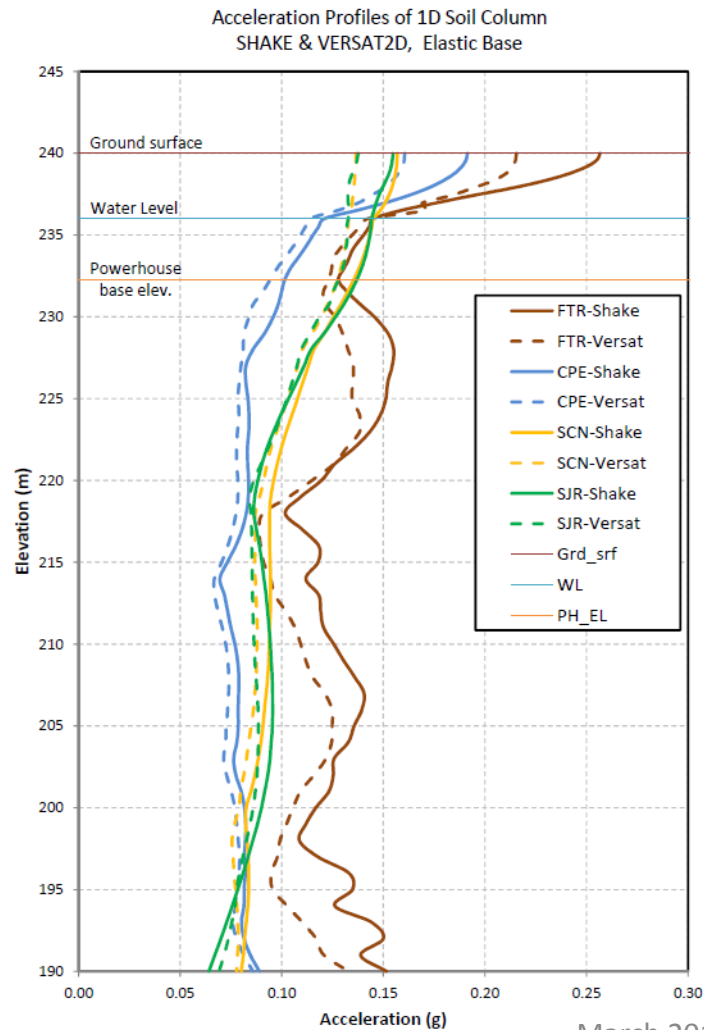
Table 2.3 Soil Stiffness and Strength Parameters for VERSAT-1D (*viscous damping 0.5% for mass & stiffness*)

Layer	VERSAT-1D Soil Zone #	Soil Layer Description	G_{max} (kPa)	K_G	c (kPa)	ϕ (°)	R_f
1a	M1	Wet Loose to Compact Sand and Gravel (a.wt)	50887	502	0	3	1500
1b	M2	Saturated Layer 1a (b.wt)	194495	1920	0	35	1500
3	M3	Compact Gravel to Gravel	345770	3413	0	35	1500
4	M4	Very Stiff to Hard Clay and Silt	269505	2660	30	25	750
Elastic base		Very Dense/Hard Silt and Sand	Elastic base, $V_s = 450$ m/s				

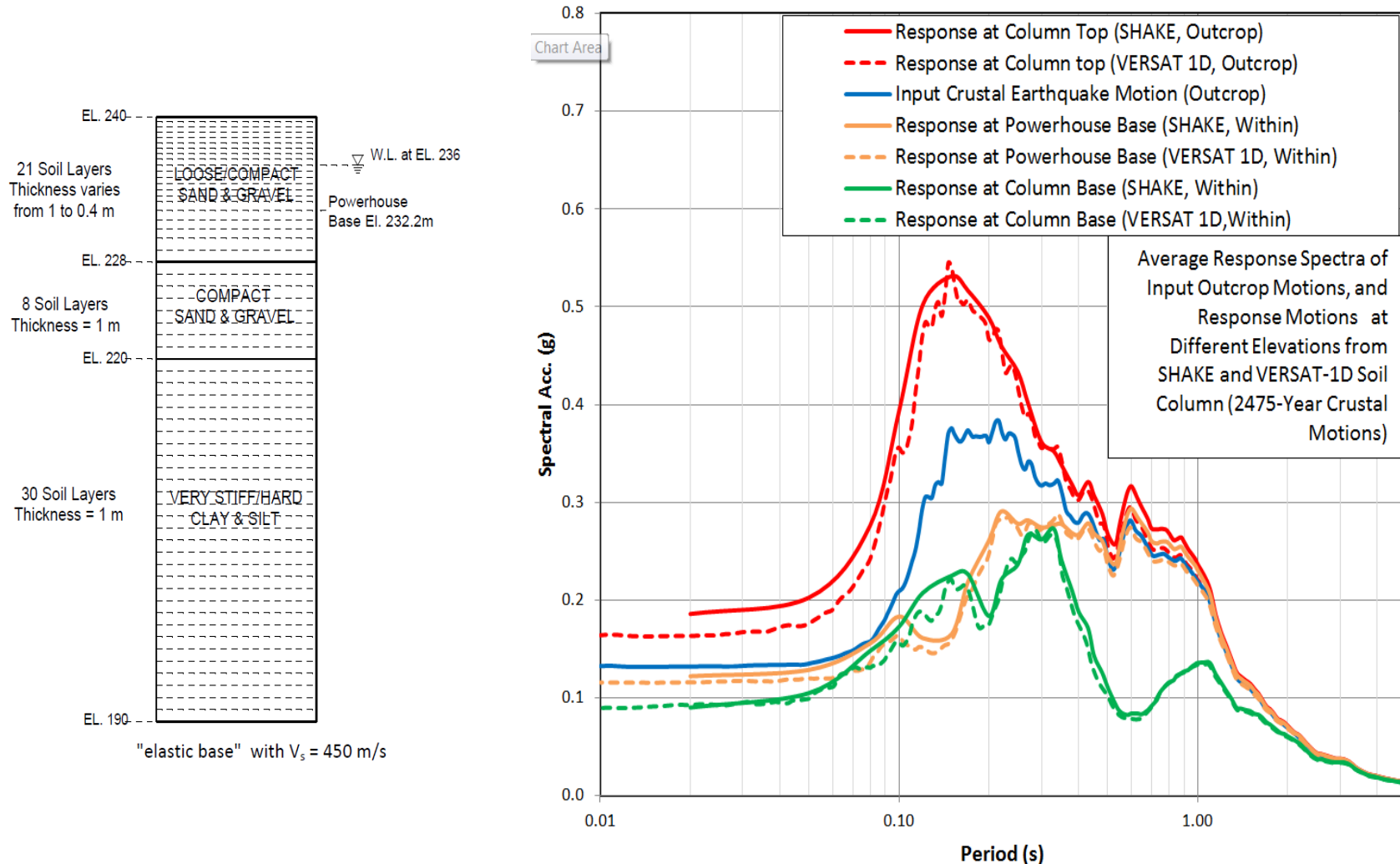
- 2.4 Example 2: Comparison between SHAKE and VERSAT-1D at low-moderate level of earthquake shaking:
 G/G_{max} and damping curves used in SHAKE analyses



- 2.4 Example 2 Comparison between SHAKE and VERSAT-1D:
RESULTS - at low-moderate level of earthquake shaking, *SHAKE equivalent linear approximation is able to produce very good representation of true soil nonlinear hysteresis behavior*



- 2.4 Example 2 Comparison between SHAKE and VERSAT-1D:
RESULTS for average of 7 crustal EQ motions - at low-moderate level of earthquake shaking, *SHAKE equivalent linear approximation is able to produce very good representation of true soil nonlinear hysteresis behavior.*



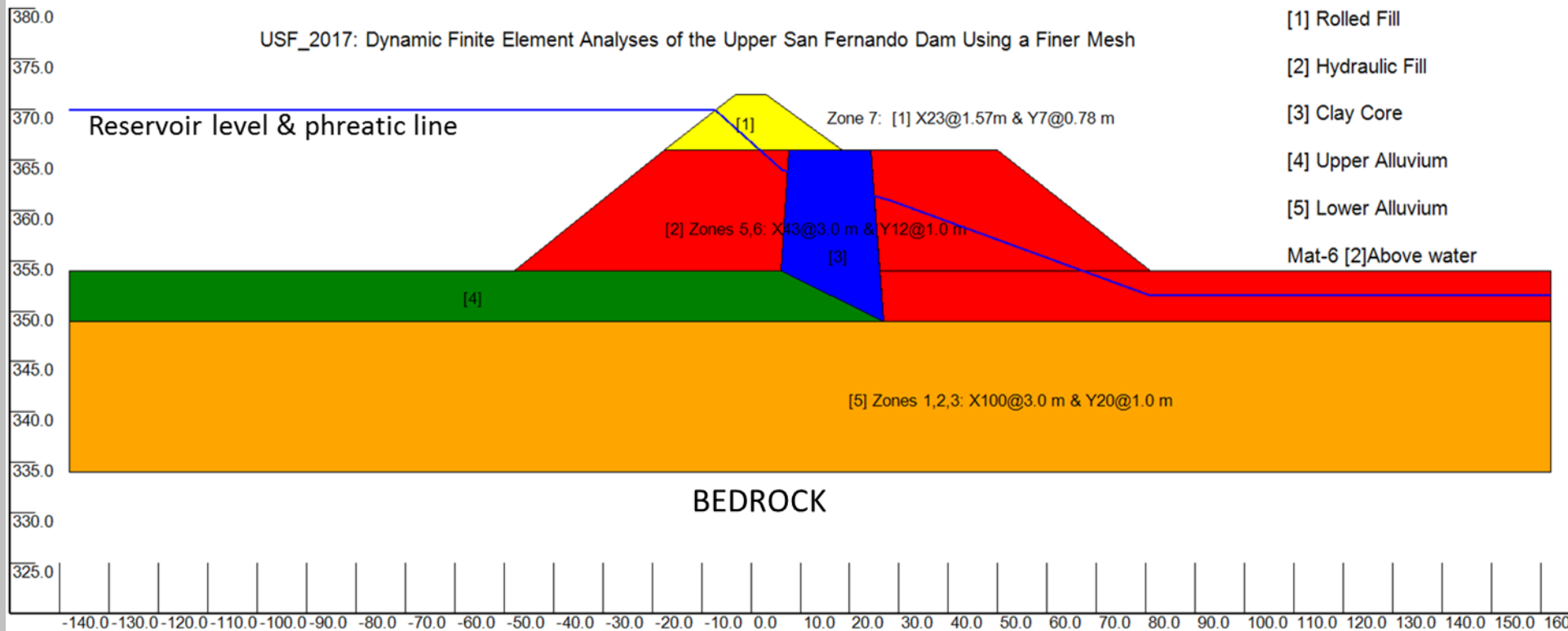
Appendix B: VERSAT-2D Dynamic Analyses of Upper San Fernando Dam

(see Volume 2 User Manual for Step-by-Step Preparation of the Model)



- **4.1 Case History Study by Finite Element Approach**
for Dynamic Analysis Of the Upper San Fernando Dam Under The 1971 San Fernando Earthquake: Pacoima Record (PGA 0.6g) (Wu 2001)

- [1] Model creation:



- **4.1 Case History Study by Finite Element Approach Analysis Of Upper San Fernando Dam Under The 1971 San Fernando Earthquake**
- [1] Model creation:

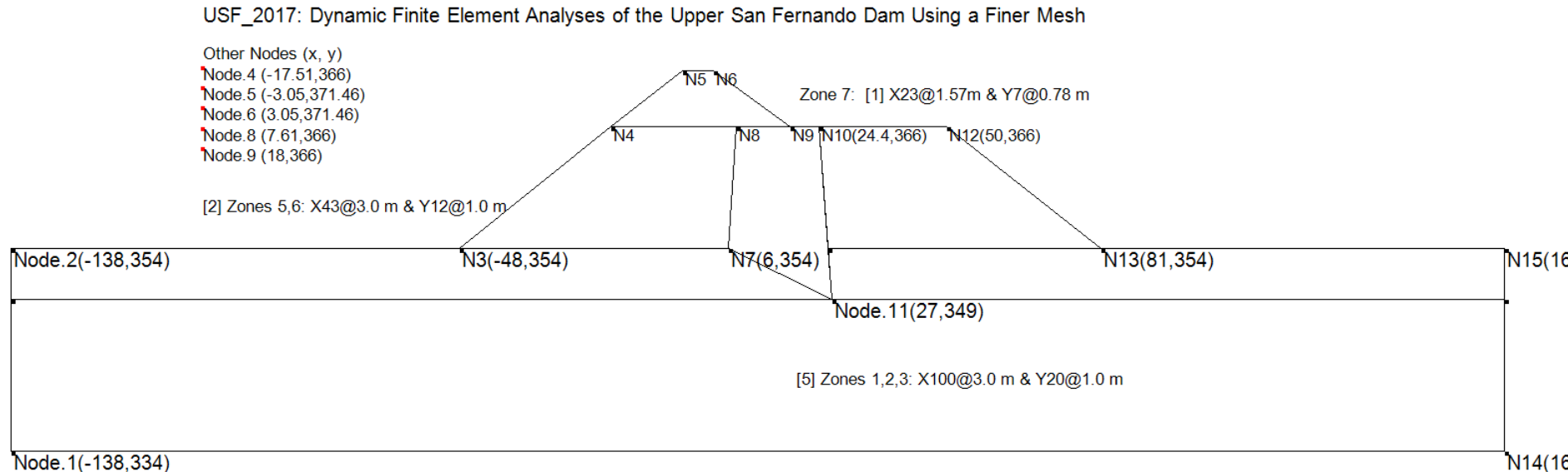
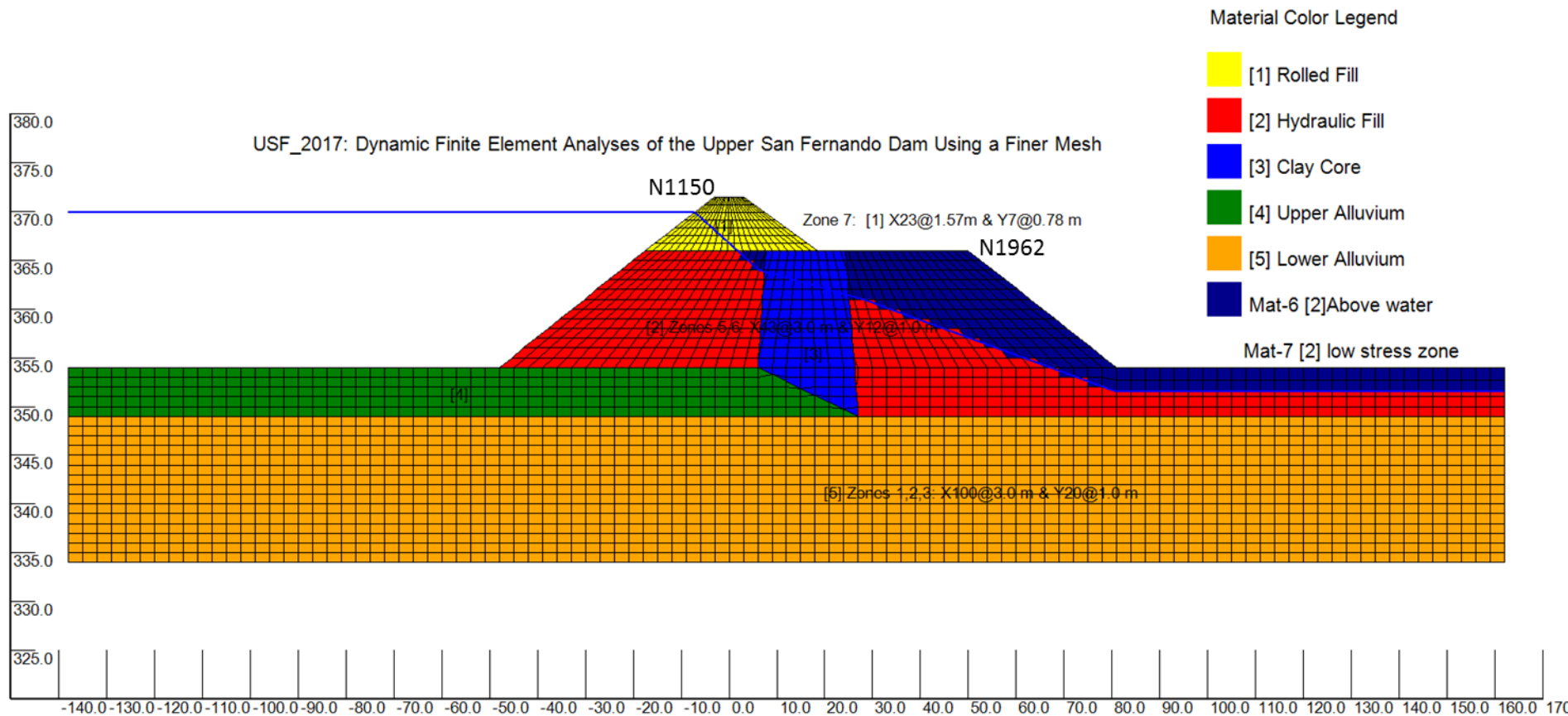


Table 1. Soil stiffness and strength parameters of the Upper San Fernando Dam (Seed et al. 1973).

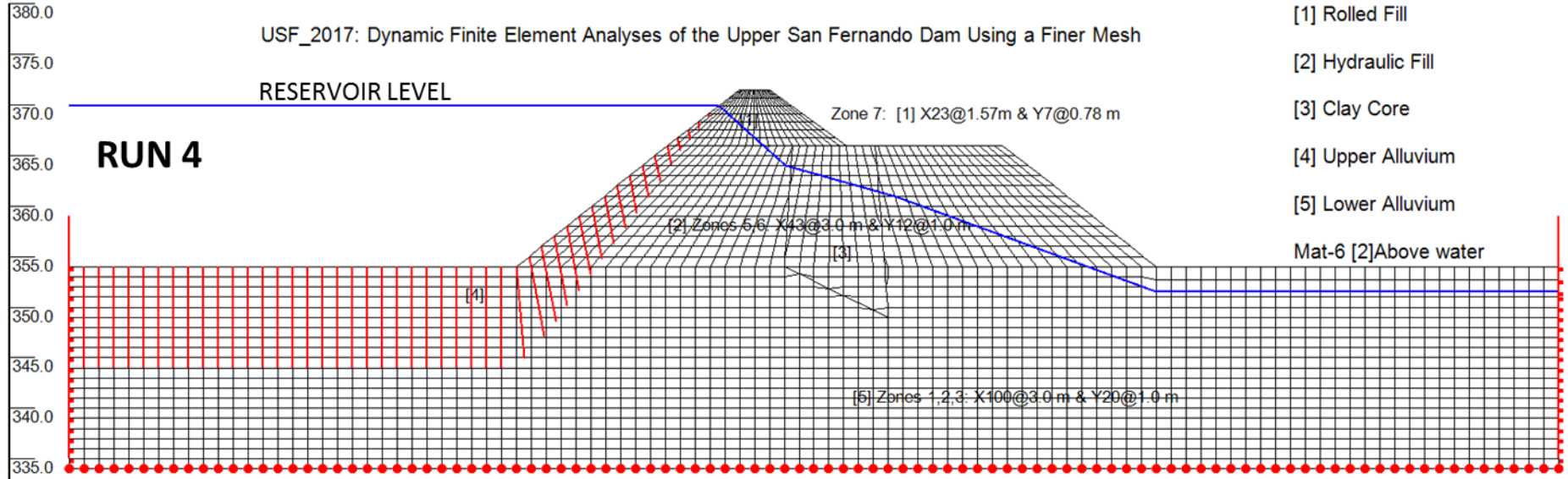
Soil unit	Soil material	Unit weight (kN/m ³)	Strength parameters		Stiffness parameters*		
			c' (kPa)	ϕ' (°)	K_{2max}	K_g	K_b
1	Rolled fill	22.0	124.5	25	52	1128	2821
2	Hydraulic fill	19.2	0	37	30	651	1630
3	Clay core	19.2	0	37	— [†]	651	1630
4	Upper alluvium	20.3	0	37	40	868	2170
5	Lower alluvium	20.3	0	37	110	2387	6000

*Modulus exponents ($m = n = 0.5$) were used for all soil units.

- **4.1 Case History Study by Finite Element Approach Analysis Of Upper San Fernando Dam Under The 1971 San Fernando Earthquake**
- [2] Model creation: Assign soil unit or material zones



- **4.1 Case History Study by Finite Element Approach Analysis Of Upper San Fernando Dam Under The 1971 San Fernando Earthquake**
- [3] Define soil parameters, Adjust D/S layer thickness, Set RUNs (layers, water tables, etc.), boundary, water loads



- [4] Run static analysis to obtain stresses with the existing dam
Input file: *USF_4_FINAL.sta*

- **4.1 Case History Study by Finite Element Approach Analysis Of Upper San Fernando Dam Under The 1971 San Fernando Earthquake**
- [5] Conduct the dynamic analysis:
 - setup the dynamic run in 5 minutes
 - Setup moduli and pwp parameters for dynamic
 - Create a text file for input ground motion
 - Save and run to completion in 15 minutes

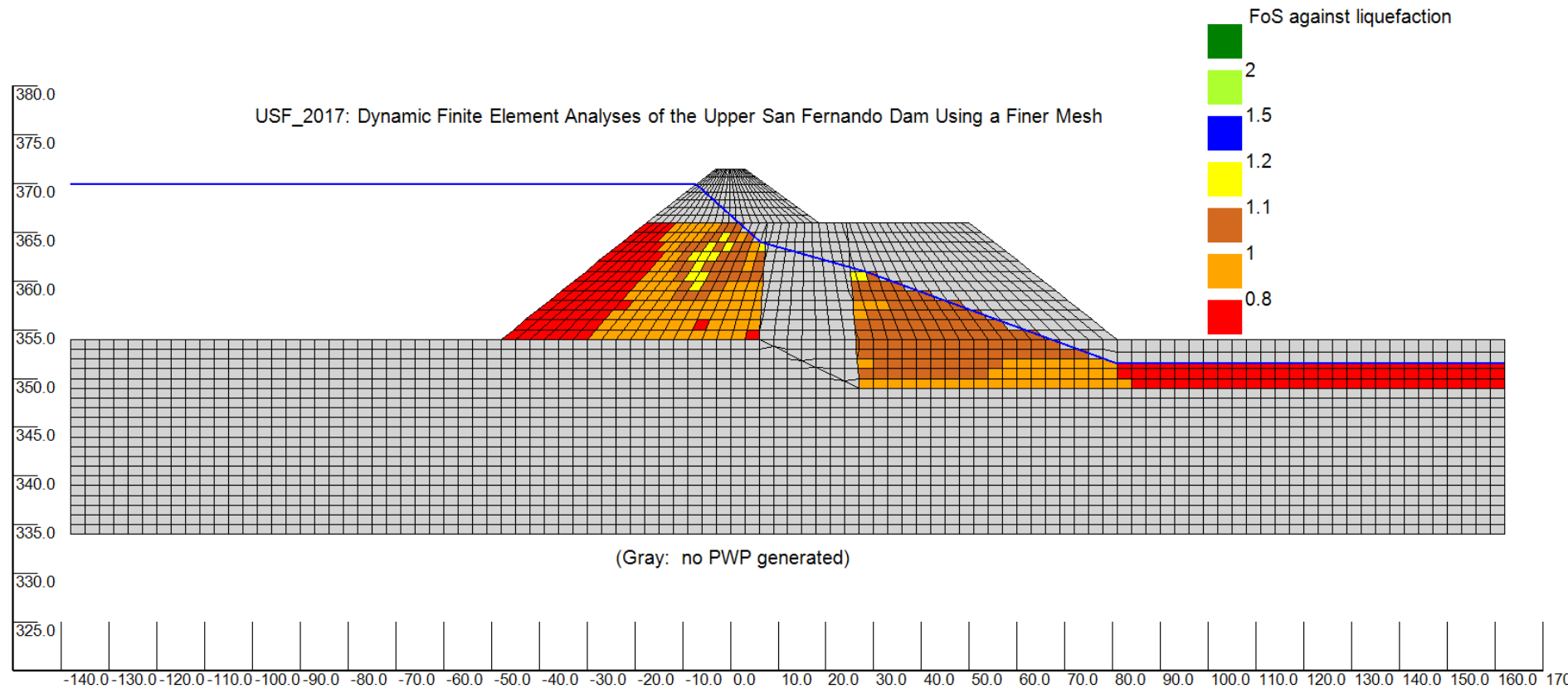
Table 4. Pore-water pressure parameters and residual strengths used in Seed et al. (1976) pore-water pressure model.

Material No.	Soil description	Equivalent $(N_1)_{60}$	CRR	α	θ	Residual strength (kPa)*	K_c LIQ
2a	Upstream hydraulic fill	14	0.154	3.0	0.1	23.0 (480)	400
2b	Downstream hydraulic fill	14	0.154	3.0	0.1	23.0 (480)	400
2c	Hydraulic fill in the downstream free field	14	0.154	3.0	0.1	14.4 (300)	400

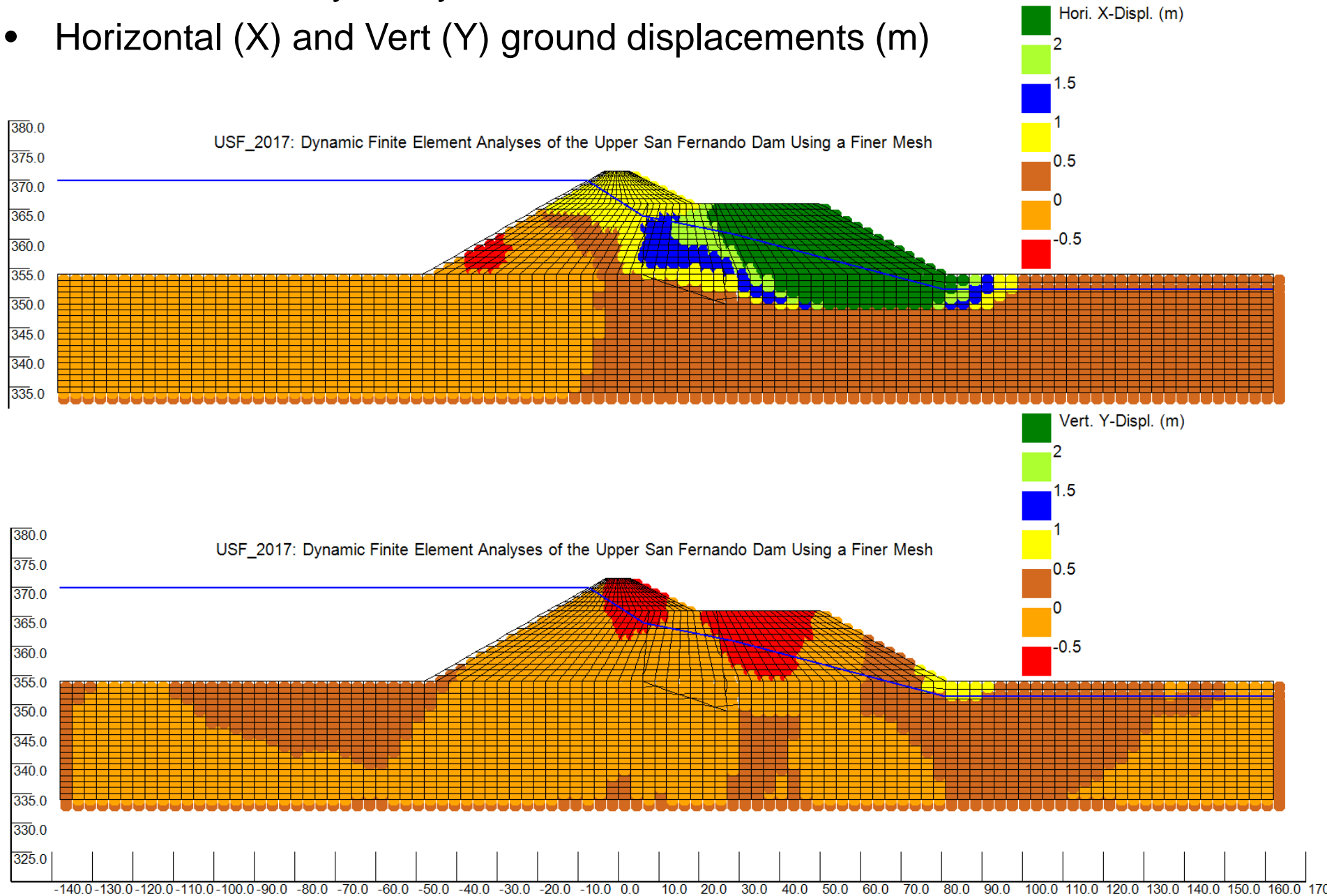
* Pounds per square feet in parentheses.

- **4.2 Case History Study – Results Shown**
- [1] Factor of Safety Against Liquefaction using Seed's PWP model

$FOS_{liq} < 1.0$ is considered liquefied in earthquake

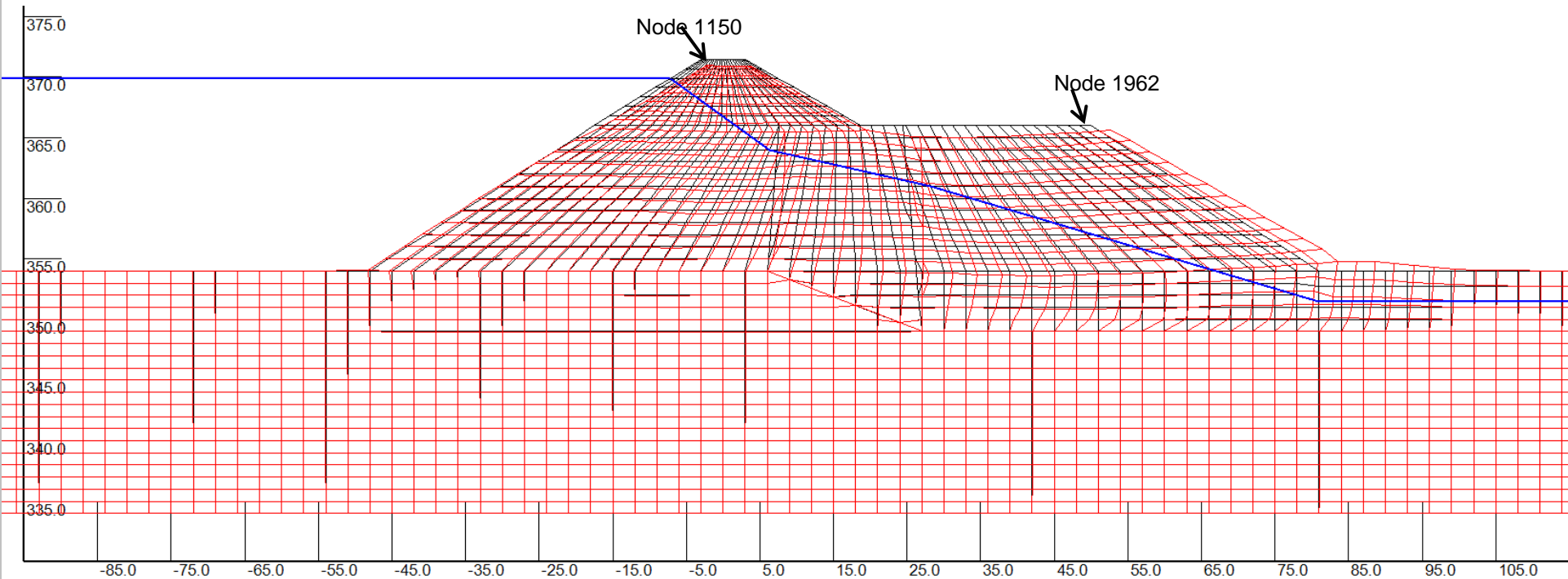


- **4.2 Case History Study – Results Shown**
- Horizontal (X) and Vert (Y) ground displacements (m)



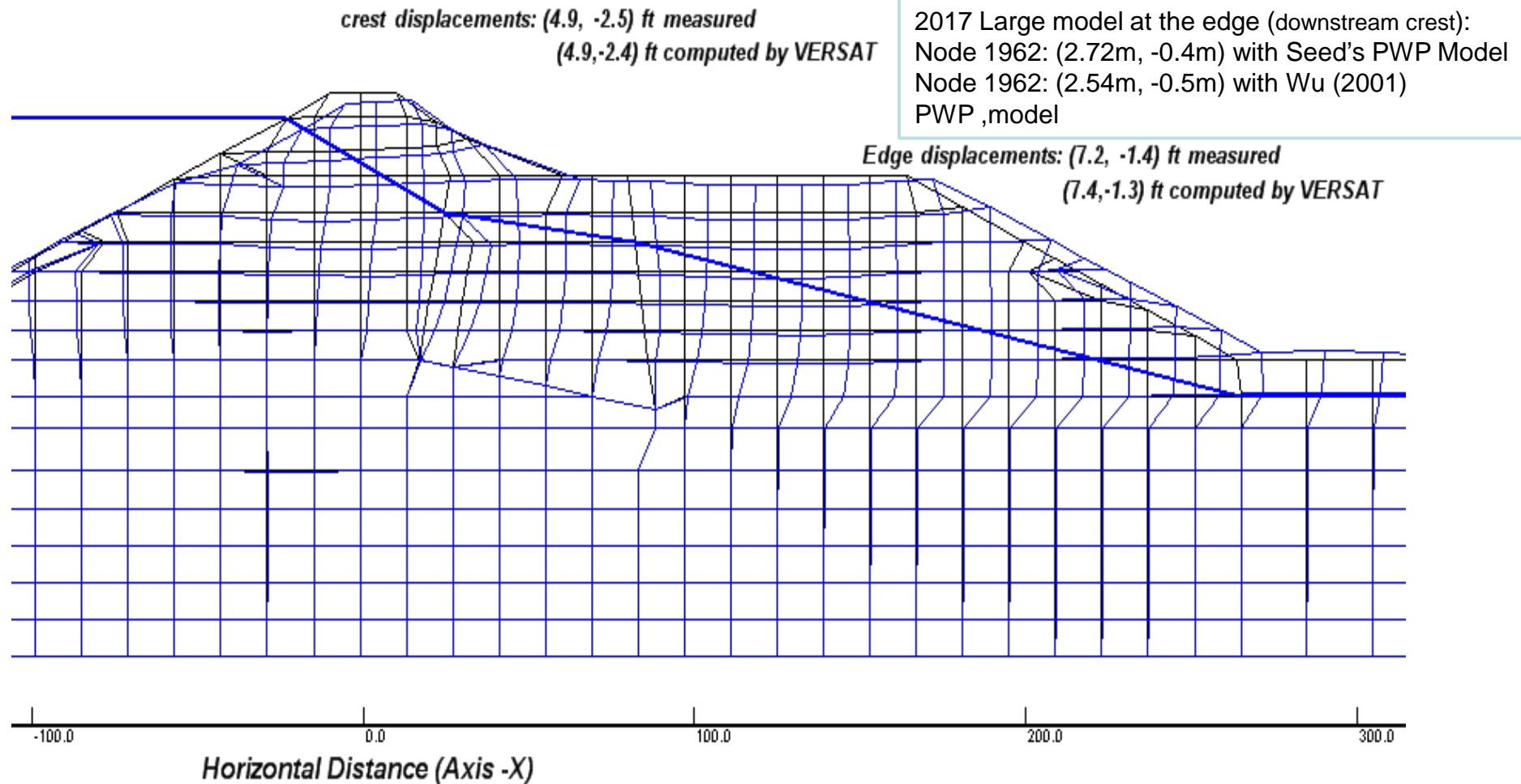
- **4.2 Case History Study – Results Shown**
2017 large model with 2835 Nodes and 2704 Elements

Deformed Ground (RED) on original ground (black) with Seed's PWP model



Note: Feb. 2017 Computed displacements at Node points:
N1150 (0.77 m, -0.52 m); N1962(2.72m, -0.40m) with Seed's PWP Model;
N1150 (0.42 m, -0.44 m); N1962(2.54m, -0.50m) using Wu(2001) PWP Model:

- **4.3 Results from Wu (2001) Small Model:**
678 nodes and 625 elements used in Wu (2001) model The dynamic analysis results are robust, consistent between 2001 small and 2017 large model (2835 Nodes and 2704 Elements).



Wu, G. 2001. Earthquake induced deformation analyses of the Upper San Fernando dam under the 1971 San Fernando earthquake. Canadian Geotechnical Journal, 38: 1-15.

[Download Now](#)